"Re-utilization of Industrial CO_2 for Algae Production Using a Phase Change Material"

Final Technical Report

Reporting Period Start Date: 1/1/10
Reporting Period End Date: 12/31/13

Brian E. Joseph
Principal Investigator
(304) 547-5800
bej@trl.com

Issued on: March 31, 2014

Department of Energy Award Number:
DE-FE0002546

Submitting Organization :
Touchstone Research Laboratory
1142 Middle Creek Road
Triadelphia, WV 26059

SUBMITTED TO:

U. S. Department of Energy
National Energy Technology Laboratory

Jason C. Hissam
Jason.Hissam@netl.doe.gov

DISCLAIMER

Abstract

This is the final report of a 36-month Phase II cooperative agreement. Under this project, Touchstone Research Laboratory (Touchstone) investigated the merits of incorporating a Phase Change Material (PCM) into an open-pond algae production system that can capture and re-use the CO_2 from a coal-fired flue gas source located in Wooster, OH. The primary objective of the project was to design, construct, and operate a series of open algae ponds that accept a slipstream of flue gas from a coal-fired source and convert a significant portion of the CO_2 to liquid biofuels, electricity, and specialty products, while demonstrating the merits of the PCM technology. Construction of the pilot facility and shakedown of the facility in Wooster, OH, was completed during the first two years, and the focus of the last year was on operations and the cultivation of algae.

During this Phase II effort a large-scale algae concentration unit from OpenAlgae was installed and utilized to continuously harvest algae from indoor raceways. An Algae Lysing Unit and Oil Recovery Unit were also received and installed. Initial parameters for lysing nanochloropsis were tested. Conditions were established that showed the lysing operation was effective at killing the algae cells. Continuous harvesting activities yielded over 200 kg algae dry weight for Ponds 1, 2 and 4. Studies were conducted to determine the effect of anaerobic digestion effluent as a nutrient source and the resulting lipid productivity of the algae. Lipid content and total fatty acids were unaffected by culture system and nutrient source, indicating that open raceway ponds fed diluted anaerobic digestion effluent can obtain similar lipid productivities to open raceway ponds using commercial nutrients.

Data were also collected with respect to the performance of the PCM material on the pilot-scale raceway ponds. Parameters such as evaporative water loss, temperature differences, and growth/productivity were tracked. The pond with the PCM material was consistently 2 to 5°C warmer than the control pond. This difference did not seem to increase significantly over time. During phase transitions for the PCM, the magnitude of the difference between the daily minimum and maximum temperatures decreased, resulting in smaller daily temperature fluctuations. A thin layer of PCM material reduced overall water loss by 74% and consistently provided algae densities that were 80% greater than the control pond.

Table of Contents

1.0 Executive Summary

The primary objective of this project was to design, construct, and operate a series of open algae ponds that accept a slipstream of flue gas from a coal-fired source and convert a significant portion of the CO_2 to liquid biofuels, electricity, and specialty products. This effort was accomplished by leveraging the successful demonstration of another Ohio Coal Development Office (OCDO)-supported technology - a coal-fired atmospheric fluidized bed combustor (AFBC) - for the supply of heat to a commercial greenhouse operation in Wooster, Ohio. A unique component of the project is that a phase change material (PCM) was utilized in the open-pond process to tackle three significant challenges facing the algae biofuels community, namely water temperature variations, water evaporation, and contamination.

The PCM technology was successfully scaled up to pilot-plant level during this Phase II project. Data were collected with respect to the performance of the PCM material on the pilot-scale raceway ponds; and parameters such as evaporative water loss, temperature differences, and growth/productivity were tracked. The pond with the PCM material was consistently 2 to 5°C warmer than the control pond. This difference did not seem to increase significantly over time. During phase transitions for the PCM, the magnitude of the difference between the daily minimum and maximum temperatures decreased resulting in smaller daily temperature fluctuations. A thin layer of PCM material reduced overall water loss by 74% and consistently provided algae densities that were 80% greater than the control pond.

Additionally, a lower-cost biological harvesting/extraction process was successfully demonstrated for the downstream process (harvesting/oil extraction) - which is currently a significant limiting economic factor to other algae producers. Parallel pilot-scale process development and testing of an anaerobic digestion process was performed by the Ohio Agricultural Research and Development Center (OARDC) in Wooster. The effluent from this process was shown to be an acceptable source of nutrients for algae growth, which should lower the ongoing operational costs.

2.0 Introduction

The utilization of algae to capture a portion of the CO_2 from coal-fired power plants has potentially significant benefits to Ohio. While Ohio has a climate that is not optimal for algae production when compared to areas like the Southwest U.S., it does have vast quantities of CO_2 and low-grade heat available from coal-fired power plants, which the Southwest lacks. By incorporating the CO_2 and the waste heat from the stacks at these sources, Ohio offers a compelling location to produce meaningful quantities of algae-based renewable energy.

The use of microalgae as a biofuel feedstock has received considerable attention in recent years and, by some accounts, is the only truly sustainable resource for replacing significant quantities of imported petroleum. Microalgae have been studied for potential biofuel use by the Department of Energy and other researchers over the past twenty years because of the potential for high oil yields as compared to other crops. The early R&D efforts focused on identification of promising strains of algae, manipulation of environmental conditions to increase lipid yields, and some limited scale-up work done in small open ponds. Just in the past several years, there has been a resurgence of research into microalgae, driven by the increase in petroleum prices and

the need for developing low-carbon energy sources. Algae can produce significantly more lipids per acre than any other source (from 5 to 30 times more, depending on the crop), can be produced on non-arable land with saline or wastewater, and do not compete as feedstock. A significant benefit is that algae consume approximately two units of carbon dioxide for every unit of biomass that is produced, making it an attractive technology for carbon capture from fossil energy combustion.

There are many companies, universities, and national laboratories involved in developing algae technologies. This work includes utilization of closed photobioreactors (PBR's), open-pond systems, or some combination of the two. Yet, the economic benefits of these approaches have not yet been proven on a larger scale. A closed system presents the best "technical" opportunity for success; however, to be proven feasible, this system has the major hurdles of capital and maintenance costs to overcome. Open-pond systems have much lower capital and maintenance costs but also produce lower yields than closed systems. If improvements to current open-pond production technologies can be achieved, then it is believed that this choice will be the dominant large-scale algae production technology going forward. However, in areas of the country where there are abundant sunlight and available land mass (such as in the desert Southwest areas) available, the daily water evaporation from open systems and temperature fluctuations in either open or closed systems will still be major hurdles to overcome. As was shown in the early Department of Energy (DOE) Aquatic Species Program (ASP) of the 1980's and 1990's, open ponds in desert climates suffered significant declines in production during hot days and cold nights. Low productivity with the open-pond systems – resulting from 1) invasion of undesirable species, 2) significant seasonal temperature fluctuations, and 3) high water evaporation rates – caused the researchers to conclude that it was not feasible when petroleum prices at the time were far less than recent prices.

This 36-month Phase II project, which was primarily funded through the DOE's NETL Industrial Carbon Capture and Sequestration program, sought to demonstrate an open-pond, algae-based technology using a PCM that could capture a portion of the carbon dioxide from the flue gas of an existing fluidized bed combustor operating on 100% Ohio coal. The site was a 300,000-sq.-ft. commercial greenhouse operation located in Wooster, Ohio, that utilized hot water from process boilers to provide heat for the production process. The atmospheric fluidized bed combustor (AFBC) was in successful operation for the past 7 years and was funded by past grants from the Department of Energy's National Energy Technology Laboratory (NETL) and the Ohio Coal Development Office (OCDO) to demonstrate a clean coal application by reducing sulfur and nitrogen emissions. A slip-stream of the flue gas from the 9.5 MM Btu/hr AFBC was routed to a series of open algae ponds covering approximately 1/2 acre that incorporated a unique phase change component that offers several significant advantages. The carbon dioxide was converted into algae biomass that was harvested for subsequent oil extraction and lipid conversion to fuel. The recovered lipids were converted into biodiesel, which was used by the host site as fuel. The byproduct algae residuals were used to perform anaerobic digestion trials at the nearby Ohio State University's OARDC. The biomethane that was produced was combusted for electricity generation, while the liquid effluent containing the noncarbon nutrients was recycled back to the algae growth process. The key objectives of the project were to (1) demonstrate the efficiency and benefits of a carbon capture and re-use process by growing algae in open ponds using a PCM technology at the pilot scale, (2) determine the projected capital and operating costs for scaled

systems using this approach, and (3) determine the economic viability of the system at scale, including the co-product value (liquid fuel and electricity).

The continued use of Ohio's coal for inexpensive power generation depends on technology development that can mitigate carbon emissions. This project had a direct impact on the carbon emissions of one small coal-fired source in Ohio and demonstratef that, upon scale-up, it may find applicability across Ohio and the nation. The future of Ohio's coal-based generation and, ultimately, the consumption of some 20 million tons of Ohio-mined coal per year could be impacted as a result of carbon emissions. As a result of this project, a viable method for utilizing carbon emissions from coal-fired sources was demonstrated, and a unique system can then be commercialized, ultimately leading to job creation in Ohio through adoption of the process near coal-fired sources as well as in the manufacturing and servicing of the process equipment and technology to customers nationwide. Significant algae research and development for biofuels production is occurring in the southern portions of the United States where more abundant sunshine and warmer temperatures can be more productive. The PCM concept will not only benefit algae production in the cooler climate of Ohio but will also benefit the algae production of other companies nationwide, thus offering the possibility of establishing a manufacturing base for this technology in Ohio. As a result of this project, a total of 2 new jobs were created in Ohio, not including temporary construction jobs.

3.0 Technical Discussion

The technical efforts under this program were focused on five main activities: development of the PCM material, development of a low-cost algae feedstock based on algae residuals, implementation of extraction and conversion processes, pilot plant design and construction, and pilot plant operation. Each of these is discussed in detail below.

3.1 Development of PCM Technology

In order to cost-effectively evaluate the system performance based on the pond geometry, fluid flow, temperature, light intensity, and nutrient concentrations, a computational fluid dynamics model was introduced to simulate various operating conditions. A particular area of interest was the self-shading that occurs in high cell concentrations and its effect on system productivity. The flow modeling software ANSYS Fluent was used to design and solve the proposed model in regards to fluid flow, heat transfer, and also nutrient balance (**Figure 1**). The integration of physical, thermochemical, and biological effects was hypothesized to predict the space- and time-dependent algal growth in the demonstration scale pond. Simulated results were proposed to be compared with the distributions of light intensity, temperature, nutrient concentration, and algal biomass acquired from four industrial-scale raceway ponds constructed for the growth of *Nannochloropsis salina*.

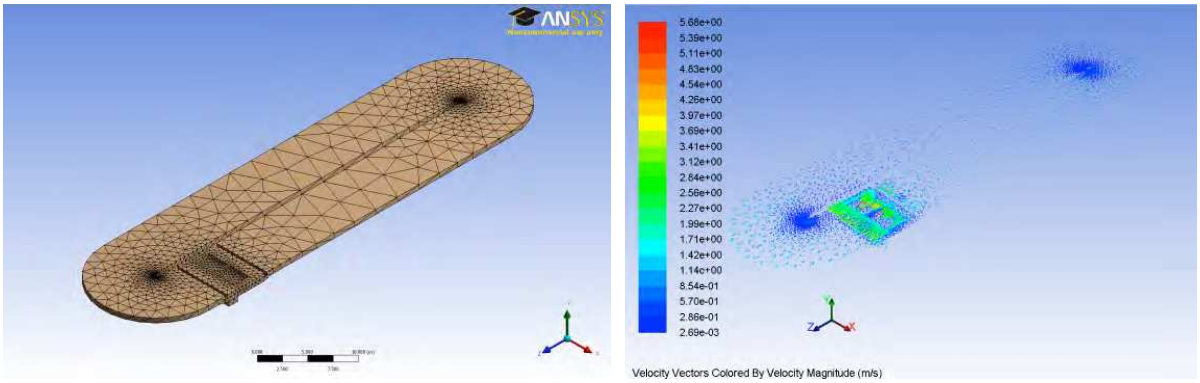

Figure 1. (a) Mesh generated from microalgal pond fluid volume, and (b) fluid velocity profile generated with CFD software (ANSYS FLUENT)

This model was used as the starting point for the design and build activities and was to be validated once the operation is up and running.

Touchstone completed the design, fabrication, installation, and operation of sub-scale raceway tanks and continuous centrifuge at its Wooster facility to further optimize the design of the PCM approach. The tanks were approximately 12 ft. in length and contained 500 gallons of water each (**Figure 2**). The algae strain utilized had been grown and harvested periodically for larger volume analytical testing and oil-extraction studies. Refinement of the PCM approach and prototypes of a system-level design to incorporate the technology into large-scale open raceways was performed.

Figure 2. Raceways in operation at Cedar Lane Farms and small continuous harvesting centrifuge

An important function of this task was the determination and selection of the PCM formulation and thickness, such that this design could be used in the large, open-pond systems that were constructed in Subphase 2b. The PCM utilized consisted of a binary mixture of the normal-paraffins and other phase change materials. These materials were identified by others as useful phase change materials, due to their high latent heat storage capacity, inertness, and relative cost. The temperature at which a binary mixture of these materials changes from a liquid to a solid (thus releasing stored heat) can be easily altered by manipulating the mixture ratio. Based on previous research, and summarized in the graph in **Figure 3**, the solidification temperature can be infinitely varied between 2°C and 18°C as needed. [Bo, Gustafsson, Setterwall, *Energy* 24 (1999) 1015-1028].

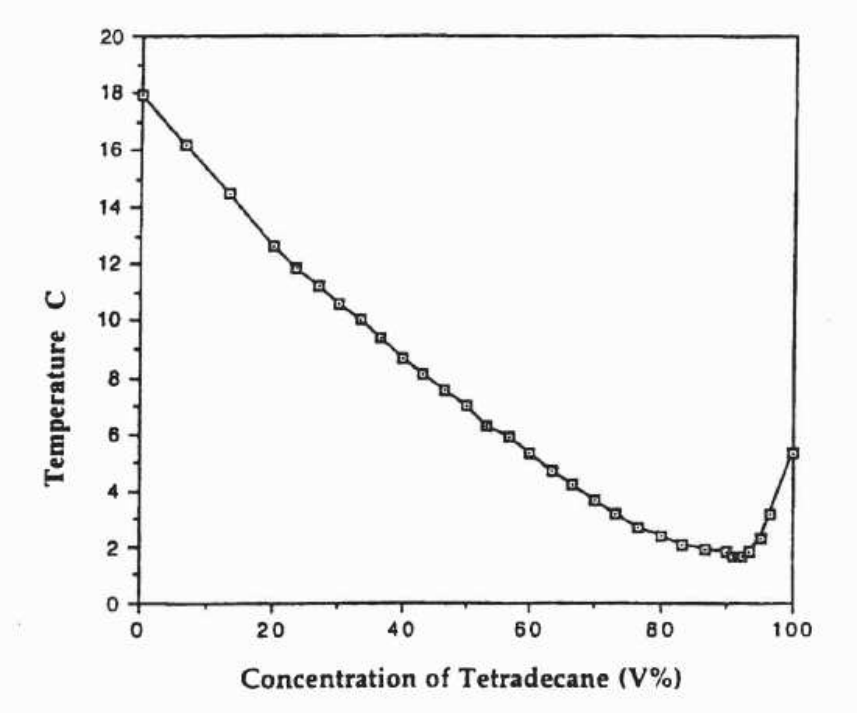

Figure 3. Solidification temperature of a binary mixture of phase change materials

3.2 Algae Feedstock Development

Previous experiments by others have shown that whole algal biomass can be anaerobically digested, but the biogas yield was shown to be lower than that of other feedstocks because of high ammonia content, increase in pH, and the recalcitrant nature of microalgal cell walls (Golueke et al., 1957). A possible method to mitigate the excessive ammonia production from protein degradation would be to supplement the digester medium with a high-carbon and low-nitrogen substrate and, consequently, increase the originally low carbon-to-nitrogen (C/N) ratio to an optimal value (Yen and Brune, 2007). This task was used to research the addition of fat, oil and grease (FOG) waste to ABR of *Nannochloropsis salina* for enhancing the degradation of algal biomass as well as for increasing the methane production efficiency per reactor volume.

Touchstone supplied a number of aqueous algae paste samples to SRS for evaluating the wet algae fractionation process. **Figure 4** contains the block process flow diagram of the SRS Algafrac process, which was followed to process algae samples in both bench unit (for small samples) and pilot facility (for large samples).

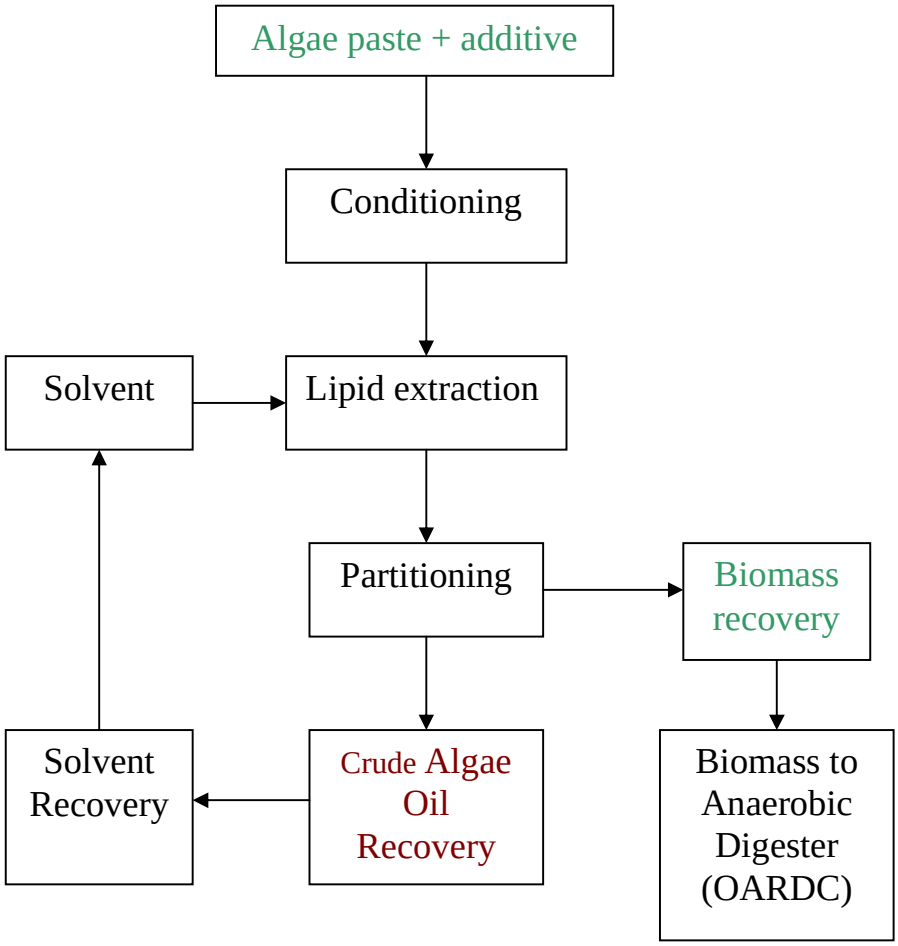

Figure 4. SRS Algafrac process flow

Process data was generated from the pilot unit operations, and process engineering calculations were carried out to study the following:

Process reliability: Most of the algae samples were processed with ease, and it was expected that more processing experiments would result in a reliable process to produce algae lipids and other fractions.

Heat and mass balance: Detailed calculations were made, and it was observed that an energy-efficient fractionation process could be developed for the samples processed. Fractionation energy consumption was calculated as per following (**Table 1**):

Table 1. Calculated energy consumption for the algae fractionation/product conversion

Algae oil yield w/w%	Thermal energy Kcal/ Kg algae oil	Electrical energy Kcal/ Kg algae oil	Total Energy Kcal/ Kg algae oil
28.5	2793	247	3040

31.1	2560	226	2786
62.4	1279	112	1391

Operating cost: Operating cost was calculated with $5/MMBTU being the energy cost. Other consumables cost was assumed at broad commercial cost.
Operating costs were calculated as per following (**Table 2**):

Table 2. Calculated operating costs for the algae fractionation/product conversion

Algae oil yield w/w%	Operating raw and energy cost $/gallon algae oil
28.5	0.31
31.1	0.29
62.4	0.18

Scaled-up pilot plant design: Detailed process engineering was developed to process anticipated algae volumes from the ponds planned to be built during Subphase 2b. Equipment sizing calculations were carried out to evaluate current pilot plant capacity. It was expected that extra capacity would need to be created in the near future to process the planned volumes of algae.

Anticipated pilot plant modifications: Mechanical designs of additional pilot equipment were prepared, and a number of additional pieces of equipment were modified and installed in anticipation of the start of Subphase 2b.

Process up-gradation: Proof-of-concept experiments were carried out to improve processing of algae and to reduce energy consumption. The results were encouraging, and a detailed process flow diagram of a "Gen II" unit was built. Further work to test this process was begun.

Fuel up-gradation: Experiments were made to recover useful triglyceride factions from crude algae oil, and initial experiments produced promising results. Detailed technical evaluation was carried out to select the most efficient process to upgrade crude algae oil. Kilogram quantities of extracted crude algae oil from Touchstone samples were processed, and a clarified triglyceride stream was produced. A process was developed to convert this triglyceride fraction into esters representing a quality algae biodiesel.

Processed biomass recycles: Spent algae biomass was recovered and sent to OARDC to evaluate its use as a feedstock for anaerobic digestion.

OARDC research on the co-digestion of algae biomass residue (ABR) and fat, oil, grease waste (FOG) under this task have shown that optimal methane yields were obtained with co-digestion when compared to the individual digestions of ABR and FOG. Co-digestion also allowed for a

higher organic loading rate (OLR), up to 3 g volatile solids (VS)/L·d, thus displaying a techno-economic benefit for the digester scale-up.

The objectives of this task were to:

- Identify any favorable substrate-to-inoculum mixing ratios to enhance the anaerobic digestion of algal sludge after lipid extraction,
- Observe the effect of the co-digestion of algal sludge and fat, oil, and grease (FOG) compared to the anaerobic digestion (AD) of the individual substrates, and
- Identify favorable conditions for the digestion of algal sludge and its co-digestion with a carbon-rich fat, oil, and grease (FOG) mixture at different substrate-to-inoculum ratios.

2-L batch reactors, each with a working volume of 1.5 L, were prepared as shown in **Figure 5**. Post-extraction algal sludge (SRS Energy, Dexter, MI) and FOG (Hardy, OH) were used as substrate. Lipids were separated from algae grown in photobioreactors through electro-treatment and acid treatment and were extracted with hexane. The AD inoculum was the effluent from a commercial-scale digester (quasar, Zanesville, OH). **Table 3** shows the total solids (TS), volatile solids (VS), carbon-to-nitrogen ratio (C/N), and pH of the materials used in the experiment. The relative proportions of algal biomass, FOG, and inoculum were used as the variable factors during this experiment.

Table 3. Material properties of algal sludge, FOG, and inoculum

Characteristics	Algal Sludge	FOG	Inoculum
TS (%)	7.25	18.7	3.61
VS (% of TS)	64.9	87.1	55.9
C/N	6.61	16.53	6.61
pH	1.52	4.34	8.11

Figure 5. AD of algal sludge and FOG in 37°C batch reactors

Due to the low pH of the substrates (1.52 for algal sludge and 4.34 for FOG), 28% (5 M) of potassium hydroxide (KOH) was prepared to adjust the initial reactor pH to 7 and, hence, prevent any inhibition of AD due to pH. The addition of KOH differed according to the initial pH of the reactor media as well as the feed composition. Higher amounts of FOG were more difficult to adjust to pH 7, and, hence, required more addition of KOH. Reactors with more alkali will have a higher alkalinity by definition (alkalinity is equal to the stoichiometric sum of the bases in solution), and their digester performance may be affected. It should be noted that the KOH addition may have a confounding effect on the experiment, although it was too early to make any observations.

Biogas production was observed in reactors with 100% FOG and co-digestion, whereas the reactors with only algae have had no gas production since day 1. **Figure 6** shows that algae alone did not digest as well as FOG or the co-digested mixtures of algae and FOG. The methane content reached approximately 50% for the reactors containing algae, while the reactor that digested FOG alone had a methane content of 65%, shown in **Figure 7**.

Difficulty in the AD of algae may be due to the high resistance of the cell wall structure or high protein content of algal biomass. Other inhibitory factors included the initial high acidity of the algal sludge and subsequent addition of alkali, or even the high sodium content of the algae. Although the co-digestion of algae with FOG did not improve the digestion of FOG itself, there is potential that the degradation of FOG may have induced the breakdown of algae, as well. Post-digestion samples were to be analyzed for organic protein content and COD to observe the breakdown of materials in the reactors.

Figure 8 shows that a lower S/I was more favorable for optimal biogas production. Further testing can be performed in continuous reactors to observe the stability of the digestion processes.

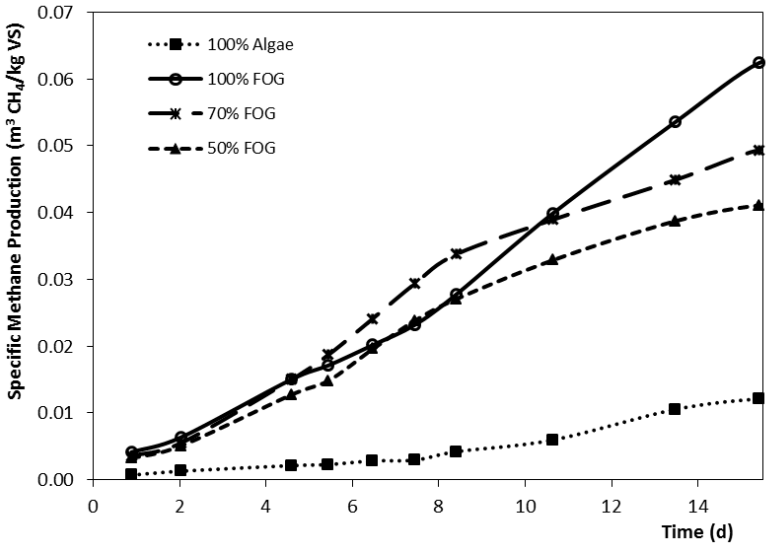

Figure 6. Specific methane production observed in AD reactors with varying feedstock compositions (S/I = 0.5)

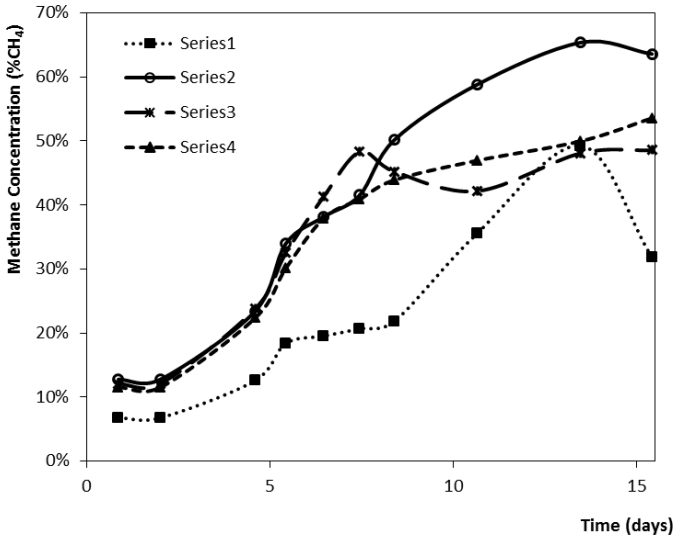

Figure 7. Methane content observed in AD reactors with varying feedstock compositions (S/I = 0.5)

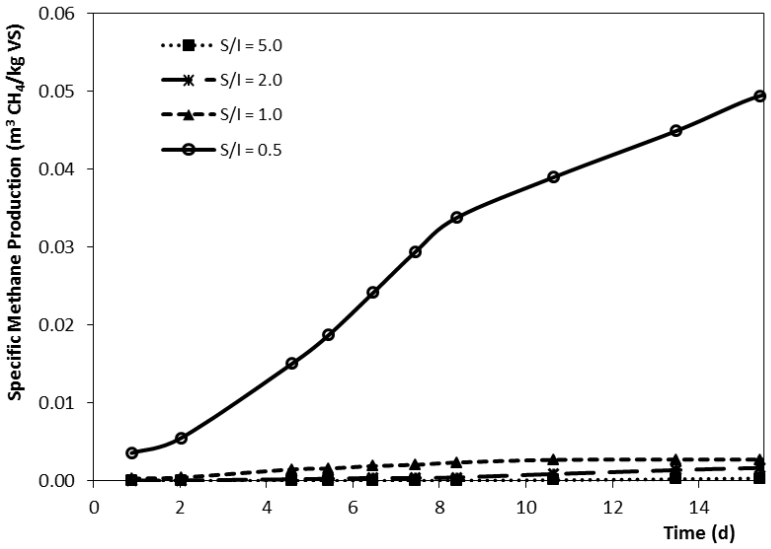

Figure 8. Specific methane production observed in the AD of 70% FOG, 30% algal sludge, with varying S/I

The C/N of algal sludge alone was 6.61. High concentrations of nitrogen relative to carbon can result in high ammonia release and volatile fatty acid (VFA) accumulation. Through the co-digestion of algae and FOG, a high-carbon feedstock, potentially toxic ammonia can be diluted, and a higher loading rate can be allowed with increased biogas yield. Samples of completed digesters were to be analyzed for total ammonia nitrogen (TAN) and VFA to observe the results of the digestion of algae and also to observe any mitigative effects that co-digestion could have. In addition, samples were to be analyzed for sodium content via ICP-MS, so that the effects of

sodium concentration on the methane production could be identified by comparing desalinated algal biomass with original samples.

Reactor design
Shown in **Figure 9**, existing 1-L batch AD reactors were modified to allow semi-continuous feeding and unloading, as well as gas sampling. Mixing was to be done by shaking the reactor and purging the sample tube daily, before reactor unloading and after feeding.

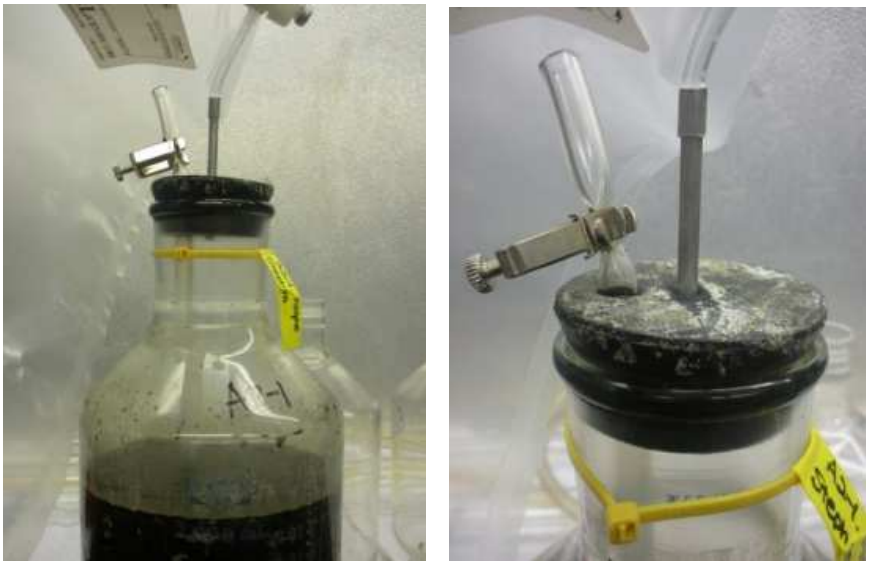

Figure 9. AD reactor modification for semi-continuous feeding of algal sludge and FOG

Specific methane yield (SMY):
As shown in **Figure 10**, co-digestion of ABR and FOG improved the stability of the AD process. Fat, oil, and grease (FOG) showed a steady methane yield of approximately 0.6 L/g VS added·day at a low organic loading rate (OLR) of 2 g VS·d (**Figure 10b**); however, higher (3 g VS/L·d or higher) organic loading rates showed eventual digester failure for the digester fed with 100% FOG, most likely due to high fatty acid production and biomass washout. The specific methane yield from 100% ABR was less than 0.3 L/g VS added·day (**Figure 10c**). Steady biogas production at higher organic loading ratio was observed with the co-digestion of ABR and FOG at ratio of 50:50, and 67:33 (**Figures 10a** and **10d**). The use of ABR alone did not result in effective biogas production, whereas the digestion of FOG was unstable at high loading rate. Co-digestion of the ABR and FOG helps mitigate the instability and results in increased biogas production.

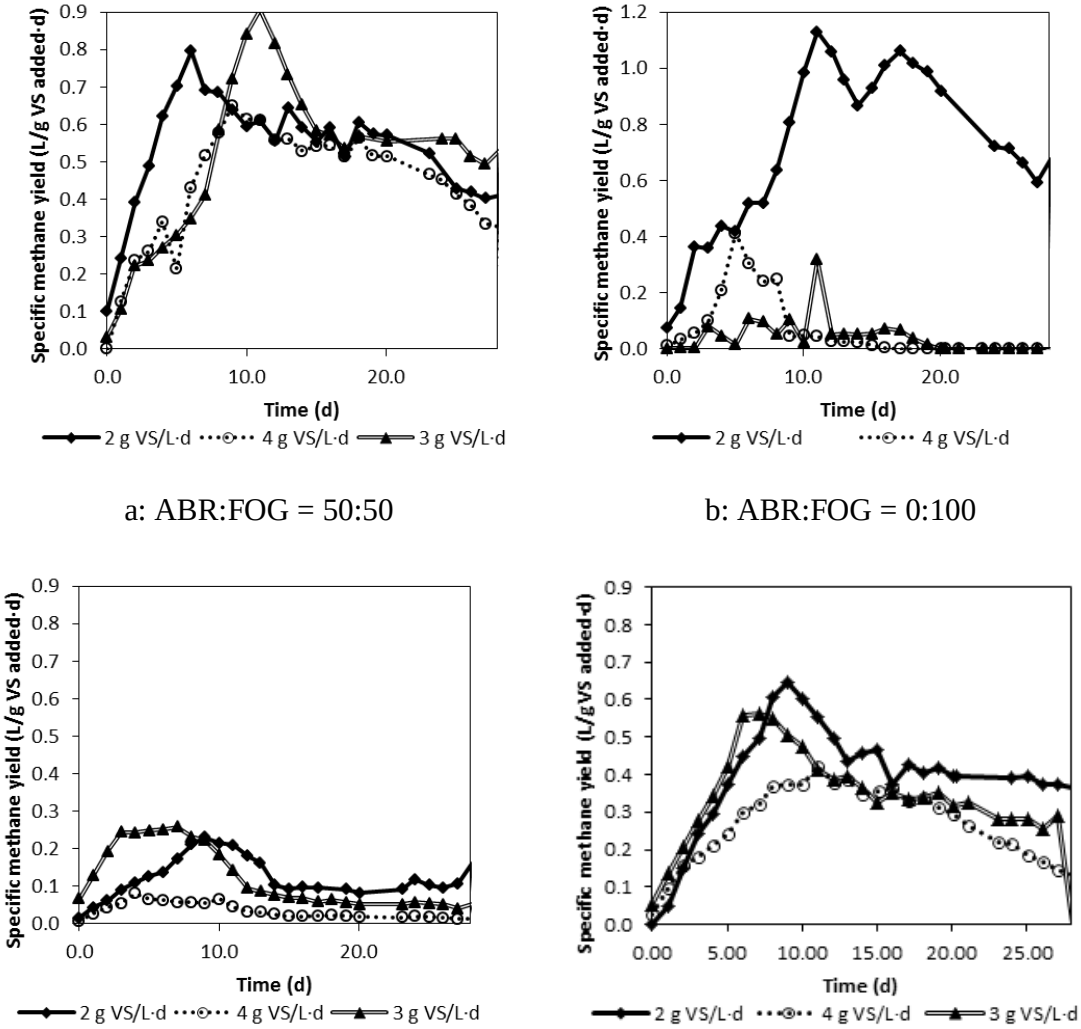

a: ABR:FOG = 50:50

b: ABR:FOG = 0:100

c: ABR:FOG = 100:0

d:ABR:FOG = 67:33

Figure 10. Specific methane yield for semi-continuous digestion of ABR, FOG, and their mixture at different organic loading rate

Methane productivity (MP):

In a scale-up perspective, the use of 50% ABR and 50% FOG shows a significantly greater volumetric methane production, in addition to a high stability. As can be seen from **Figure 11**, the highest methane productivity (methane production per working volume) was observed with the co-digestion of ABR and FOG, which was about 1.5 L/L.d at steady stage. At an organic loading rate of 2 g VS/L.d, the methane productivity of the digester with 100% FOG was about 1.31.5 L/L.d at steady stage. The methane production of the reactor with 67% of ABR was about 0.8 1.5 L/L.d on 25th day.

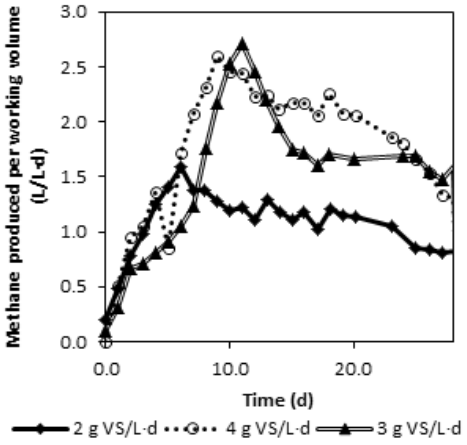

a: ABR:FOG = 50:50

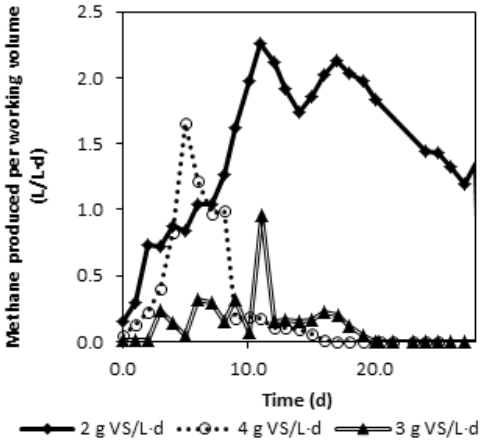

b: ABR:FOG = 0:100

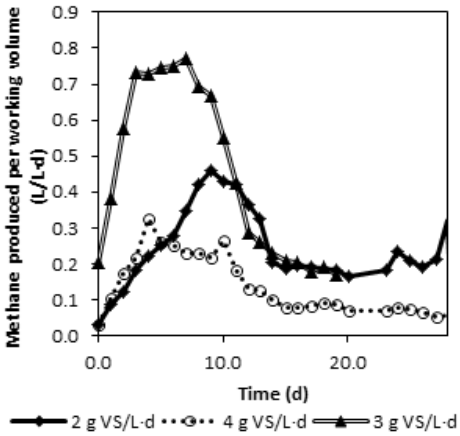

c: ABR:FOG = 100:0

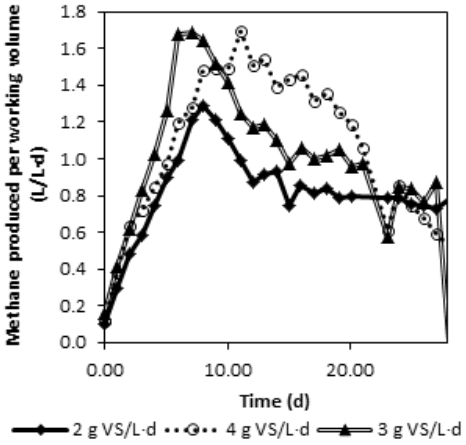

d: ABR:FOG = 67:33

Figure 11. Methane production from semi-continuous digestion of ABR, FOG, and their mixture at different organic loading rate

pH:

Observation of pH in **Figure 12** showed that there was no substantial pH drop for reactors with more than 50% of ABR in the feeding, while pH drops were observed in the other reactors. There appears to be a direct relationship between pH drop and digester failure. It can be concluded that ABR has buffer capacity that can be used as a nutrient supplement for anaerobic digesters feeding with food waste and other feedstock having high C/N ratio.

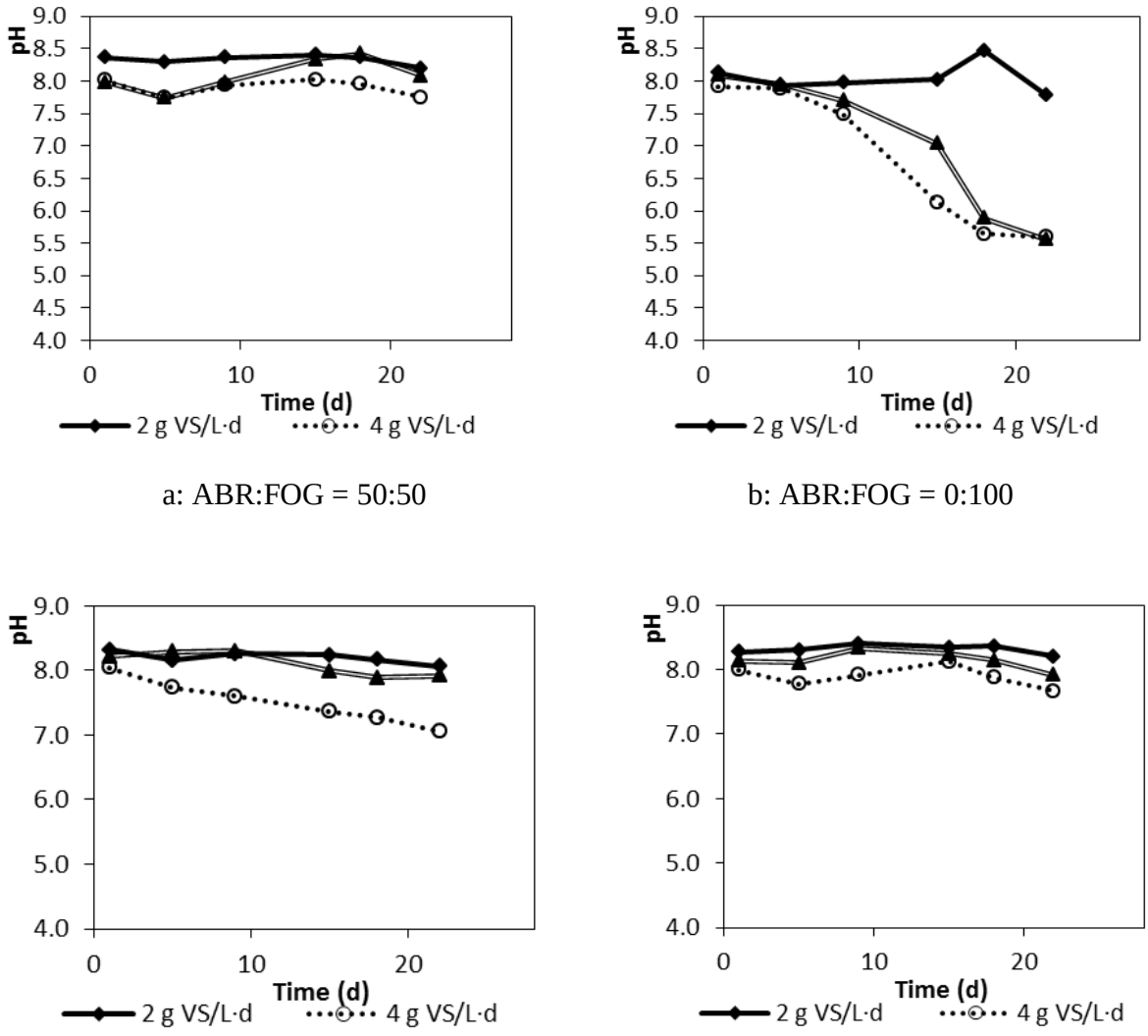

a: ABR:FOG = 50:50

b: ABR:FOG = 0:100

c: ABR:FOG = 100:0

d: ABR:FOG = 67:33

Figure 12. Variation of pH during semi-continuous AD digestion

Current tests were performed to identify the source of failure. Ammonia concentrations, VFA concentrations, degradation of nutrient components were to be analyzed to further evaluate the process. Long-term operating and monitoring of these reactors was to be continued to evaluate the performance of ABR to be used as a nutrient supplement for anaerobic digestion.

Algal oil was separated from harvested *N. salina* biomass produced by Touchstone at Cedar Lane Farms by means of electric pulsation, acid hydrolysis, and solvent recovery (SRS Energy, Dexter, MI); and the resulting ABR slurry was directly used as an AD substrate. FOG was collected from a receiving facility located in Hardy, OH. Both substrates were stored in tightly sealed plastic 5-gallon buckets at 4°C prior to use. Effluent from a commercial-scale digester fed with wastewater solids (Akron, OH) was used as the microbial consortia to degrade the organic

compounds to biogas and residuals. The characteristics of the materials used in the anaerobic co-digestion of algal biomass residue and fog, oil and grease waste are depicted in **Table 4**. Five different ABR-to-FOG percent ratios of 0:100, 33:67, 50:50, 67:33, and 0:100 were tested in this experiment.

Table 4. Characteristics of algal biomass residue

Characteristic	Unit	ABR	FOG	Inoculum
Total solids	%, w/w	14.51 ± 0.02	9.31 ± 0.08	10.05 ± 0.03
Volatile solids	% of TS, w/w	77.24 ± 0.17	85.26 ± 0.12	55.39 ± 0.14
pH		5.94 ± 0.03	4.37 ± 0.02	8.10 ± 0.03
Total carbon	% of TS, w/w	36.97 ± 0.01	-	45.67 ± 0.01
Total nitrogen	% of TS, w/w	8.38 ± 0.00	-	6.55 ± 0.01
Carbon-to-nitrogen ratio		4.41± 0.00	-	6.97± 0.01
Carbohydrates	% of TS, w/w	7.24 ± 0.00	0.596 ± 0.00	1.34 ± 0.00
Crude protein	% of TS, w/w	52.38 ± 0.00	-	-
Organic solvent extractives	% of TS, w/w	21.38 ± 0.00	82.51 ± 0.00	17.36 ± 0.00

Figure 13 shows the general experimental design of this study. Anaerobic digestion was performed in 1-L glass reactors, which were capped with rubber stoppers and constantly agitated in an Innova 43R incubated shaker (New Brunswick, Edison, NJ) at 150 rpm and 37°C. The reactors were initially filled with approximately 0.7-0.8 L of inoculum and subsequently flushed with nitrogen gas for 2 min to create an anaerobic environment. The reactors were agitated in an incubator for 3 days to acclimate the microbes to the environment before adding any substrate. A known mass of effluent was removed from each reactor daily and stored in a -20°C freezer for further analysis. Each reactor was then fed with an equal amount of substrate using a 50 mL polypropylene syringe with a Luer taper (BD, Franklin Lakes, NJ), so that the corresponding OLR would be 2, 3, 4 and 6 g VS/L·day. In order to ensure sufficient mixing at the feeding inlet and sample outlet, the syringes were purged five times before reactor unloading and after feeding. Biogas was collected from each reactor daily for volume measurement and composition analysis.

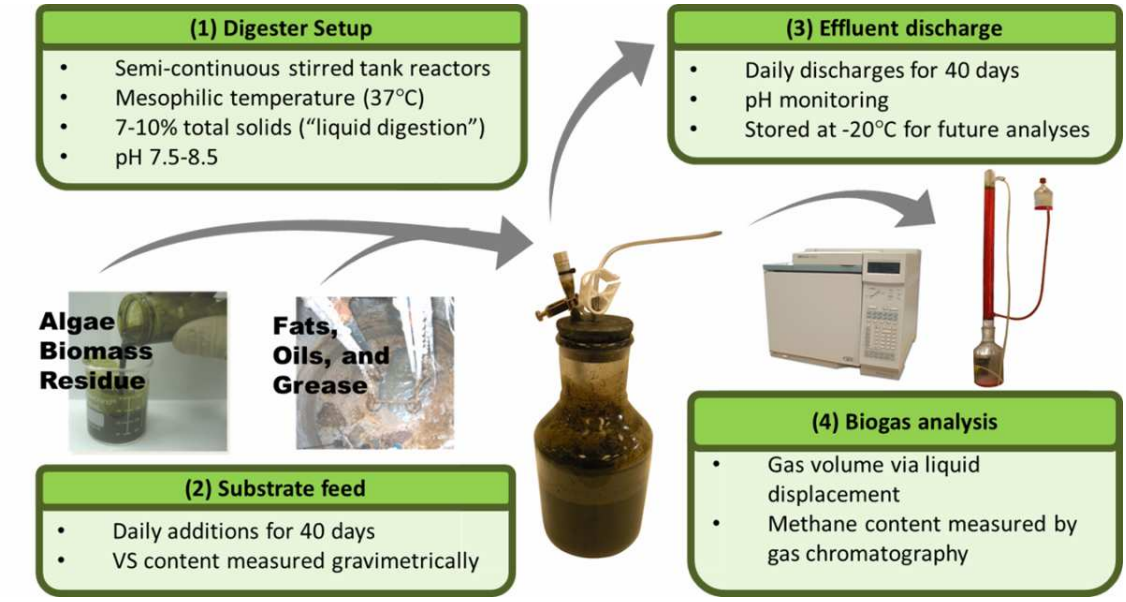

Figure 13. Experimental procedure for the semi-continuous co-digestion of ABR and FOG

Total solids (TS), volatile solids (VS), and pH of the feed material were measured according to the Standard Methods for the Examination of Water and Wastewater (APHA, 2005). One gram of each sample was placed in a clean, ignited, and tared porcelain crucible and dried in a Thelco Model 18 oven (Precision Scientific, Chennai, India) at 105°C for 4 hours. After each sample was brought to constant weight, it was cooled in a desiccator and weighed to obtain TS. Ash weight was obtained by igniting the sample in an Isotemp muffle furnace (Fisher Scientific, Dubuque, IA) at 500°C for four hours. VS was determined as the difference between the dry weight and ash weight. The pH of each reactor was measured using an AP110 portable pH meter, equipped with an Ag/AgCl reference electrode probe (Accumet, Singapore). Total carbon and nitrogen were measured with a Vario MAX CNS elemental analyzer (Elementar Analyseneyeteme GmbH, Hanau, Germany).

Carbohydrate content of the feed material were measured according to ASTM standard method E1758-01 (ASTM, 2007), where the available carbohydrates were converted to their monomeric counterparts by acid hydrolysis and then quantified by high-performance liquid chromatography (HPLC). An LC-20AB HPLC unit (Shimadzu, Columbia, MD) equipped with an Aminex® HPX-87P column (Bio-Rad Laboratories, Hercules, CA) and a refractive index detector. Distilled water was used as the mobile phase at a flow rate of 0.6 mL/min. The temperature of the column and detector were maintained at 80°C and 55°C, respectively.

Ammonia-nitrogen was determined by a procedure adapted from EPA method 350.2 (EPA, 1974) and AOAC International method 973.49 (Horwitz and Latimer, 2005). In order to liberate the ammonia, 6 N sodium hydroxide was added to each sample diluted with distilled water. The ammonia was distilled into 4% boric acid solution within a B-324 distillation unit (Büchi Labortechnik AG, Flawil, Switzerland) and titrated with 0.01 N hydrochloric acid, using a DL 22 titrator (Mettler-Toledo Inc., Columbus, OH, USA). Total crude protein was determined with

AOAC International method 2001.11 (Horwitz and Latimer, 2005). Since most proteins contain approximately 16% nitrogen, a factor of 6.25 was multiplied to the organic nitrogen content, which was estimated as the difference between total Kjeldahl nitrogen (TKN) and ammonia-nitrogen. TKN was obtained through digestion with 98% sulfuric acid in a Tecator digester (FOSS, Eden Prairie, MN, USA), followed by distillation with the B-324 and titration with the DL 22.

Solvent extractives were analyzed with a modified Bligh and Dyer (1959) method (White et al., 1979). 1.5 g of solid sample suspended in 6.5 mL of phosphate buffer (prepared with 8.7 g K_2HPO_4/L neutralized with 1 N HCl to pH 7.4) or 6.5 mL of liquid sample was mixed with 8 mL of chloroform and 16 mL of anhydrous methanol. After vortex mixing for 5 minutes, each sample was allowed to extract for a minimum of 2 hours. An additional 8 mL of chloroform and 8 mL of deionized water were added to the suspension, mixed and allowed to separate for 24 hours. The upper aqueous phase was removed by suction, and the organic phase was recovered with a Gooch filter crucible lined with filter paper. The flask holding the recovered organic phase was washed with 5 mL of chloroform. The proportions of water:methanol:chloroform were maintained to be 0.8:2:1 (v/v) for the single phase extraction and 0.9:1:1 (v/v) after separation into the second phase. The solvents were removed with an Isotemp 282A vacuum oven (Fisher Scientific, Marietta, OH) at 40°C and recovered with a condensing apparatus.

Analysis of variance (ANOVA) was performed with a significance level of 0.05 to determine all steady-state values including specific methane yield (SMY), volumetric reactor productivity (VRP), carbohydrate content, lipid content, protein content, and ammonia-nitrogen (NH_3-N) content. Response surface methodology (RSM) was used by formulating a second-order equation to describe the methane production process. All model terms were evaluated to have *p*-values less than the significance level.

Figures 14-16 show the surface response plots for SMY, VRP, and methane content, respectively. The increase in curvature along the co-digestion ratio (%ABR) axis as the OLR was increased from 2 to 6 indicated that the effect of co-digestion was more evident in higher loading rates. It can also be noted that the overall change was more drastic in OLR compared to the co-digestion ratio, indicated from the regression coefficients in the aforementioned equations.

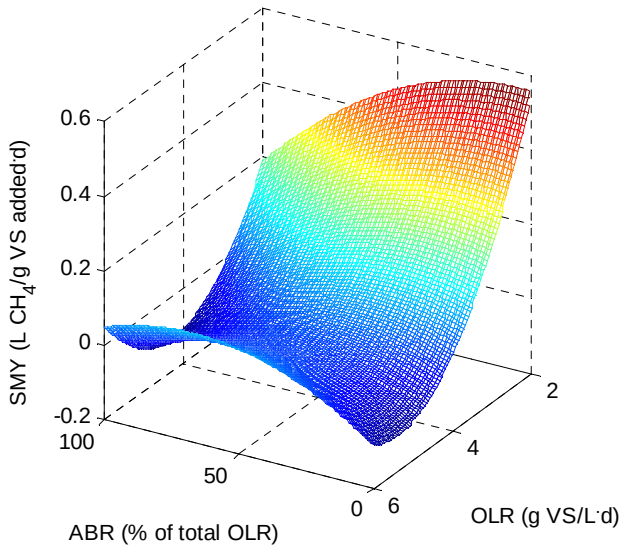

Figure 14. Response surface plot for SMY

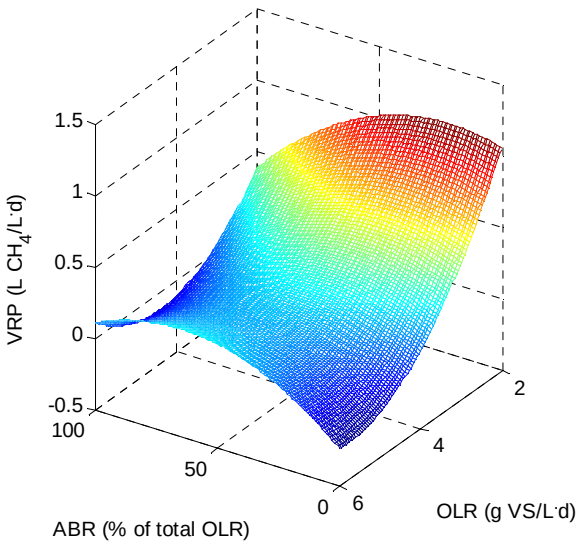

Figure 15. Response surface plot for VRP

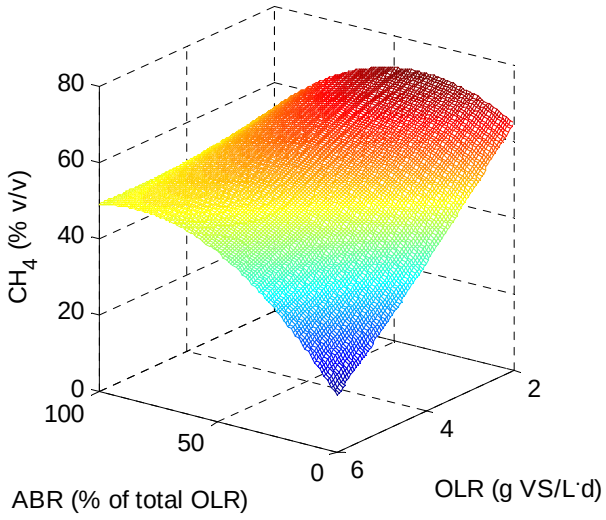

Figure 16. Response surface plot for methane yield

Figure 17 shows the change in carbohydrates, lipids, and ammonia in the digester effluent when compared to the initial feed. The increase in ammonia was assumed to correlate with the protein degradation in the anaerobic digester. It was observed that the ability to remove carbohydrates or proteins did not differ among the varying loading rates and co-digestion ratios, as the degree reductions were not statistically different among the different configurations. However, the lipid degradation performance was significantly improved when co-digesting ABR and FOG.

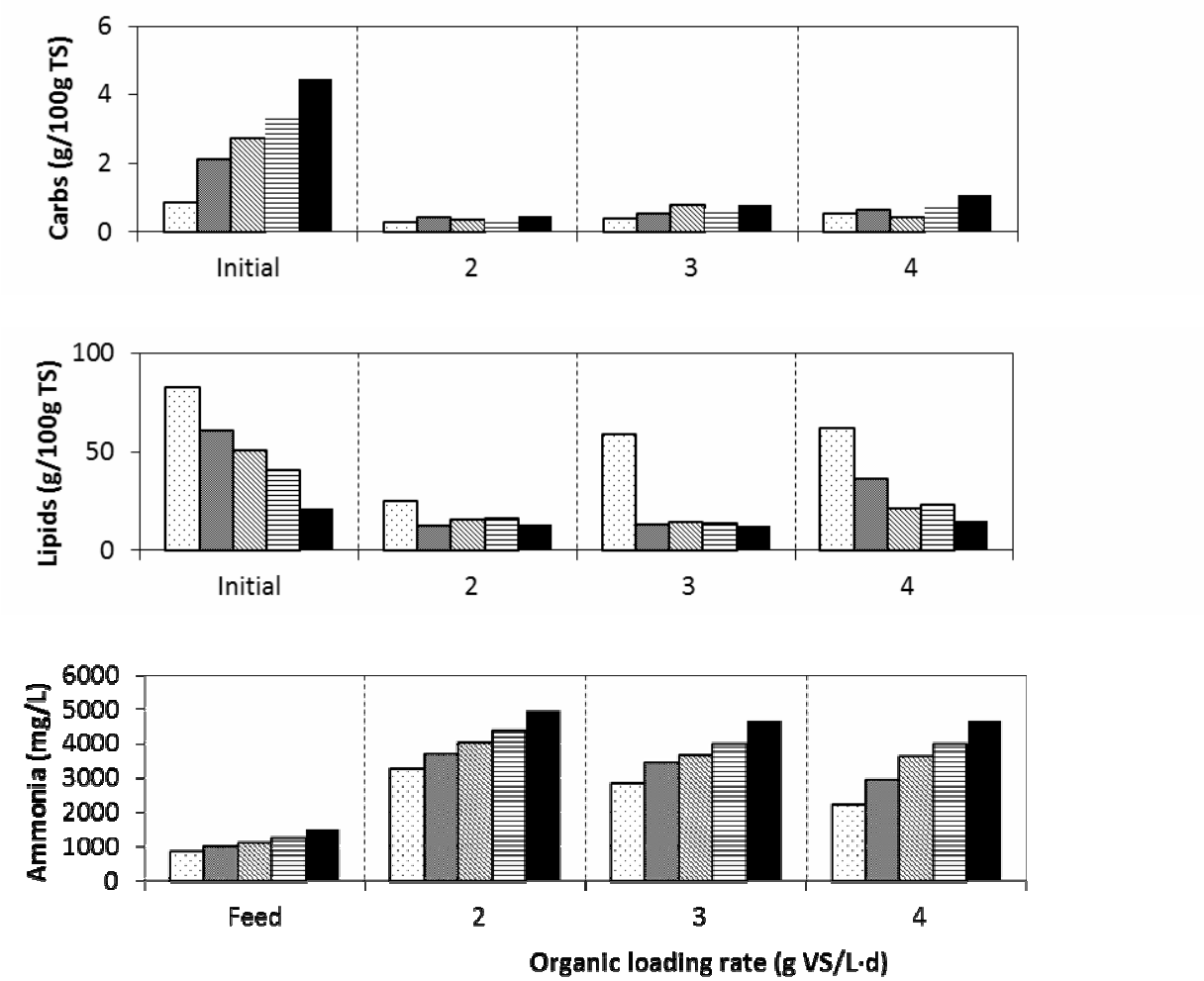

Figure 17. Carbohydrate, lipid, and ammonia concentrations in the feedstock and effluent of the anaerobic co-digestion of ABR and FOG

Based on batch experiments, *Nannochloropsis salina* was proven to be able to grow in anaerobic digestion (AD) effluent with proper dilutions for nutrients removal and lipid production. According to preliminary data, algae growth will be inhibited when the total nitrogen concentration in the culture medium is higher than 100ppm. Semi-continuous experiments were conducted with an effluent loading rate of 2%. The effects of harvesting frequency and ratio on algal biomass yield and nutrient removal efficiency were studied. The algae were cultured in 2-L glass reactors with 1-L working volume at 25°C and 150 μmol·m¯2·s¯1 continuous cool-white fluorescent light illumination. Ambient air was bubbled into reactors to supply CO_2 for algae growth and pH stabilization. All experiments were carried out in duplicate, and average values were reported. **Figures 18** and **19** show the effects of effluent loading rate on algae growth and nutrient removal rates.

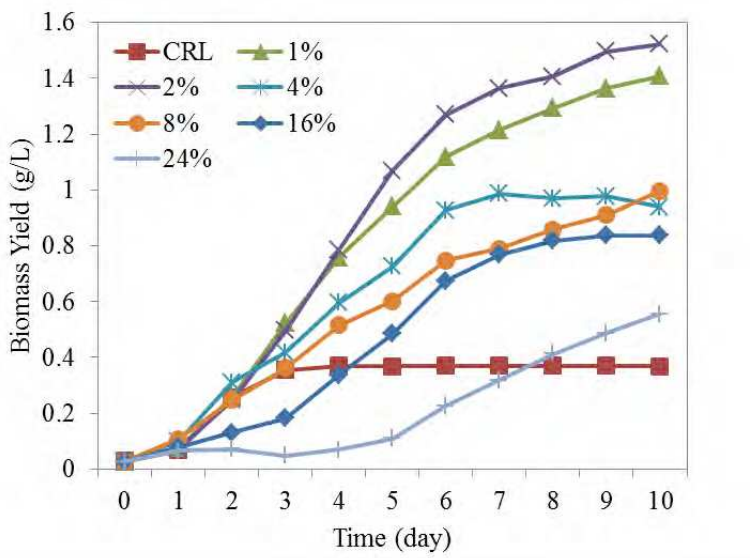

Figure 18. Algae growth curve at different effluent loading ratios in 10-day batch experiment

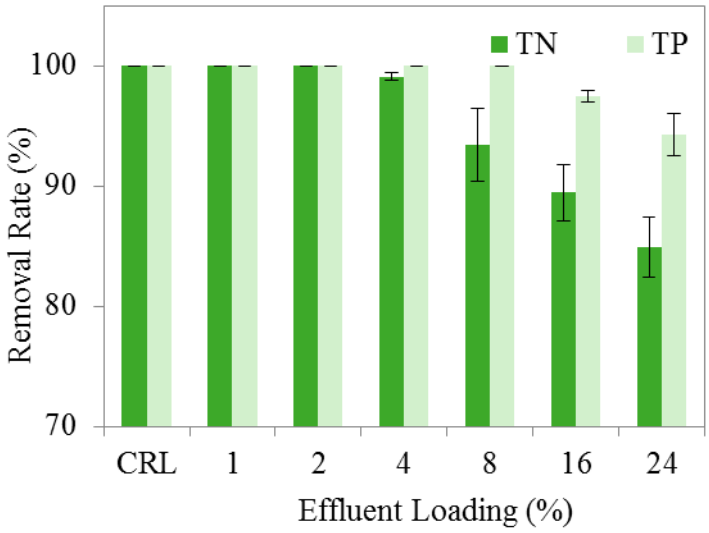

Figure 19. Total nitrogen and phosphorus removal rates by algae at different effluent loading ratios by the 10th day

Algae biomass yield was higher when grown in AD effluent than in commercial algae formula. Increasing effluent loading over 2% didn't increase the biomass yield. The nitrogen and phosphorus were totally removed at 2% and 1% loading rates. **Figures 20** and **21** show the

effects of harvesting frequency and harvesting ratio on algae biomass production and nutrient removal.

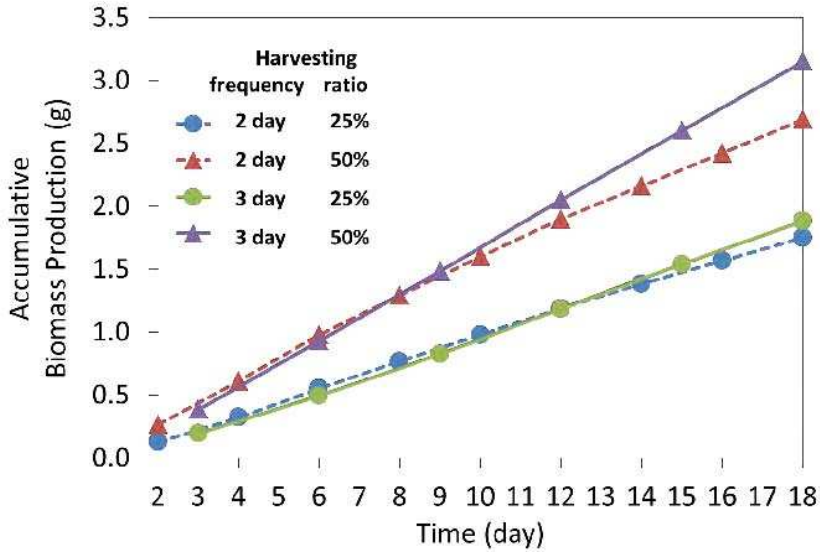

Figure 20. Accumulative biomass production at different conditions during an 18-day semi-continuous experiment

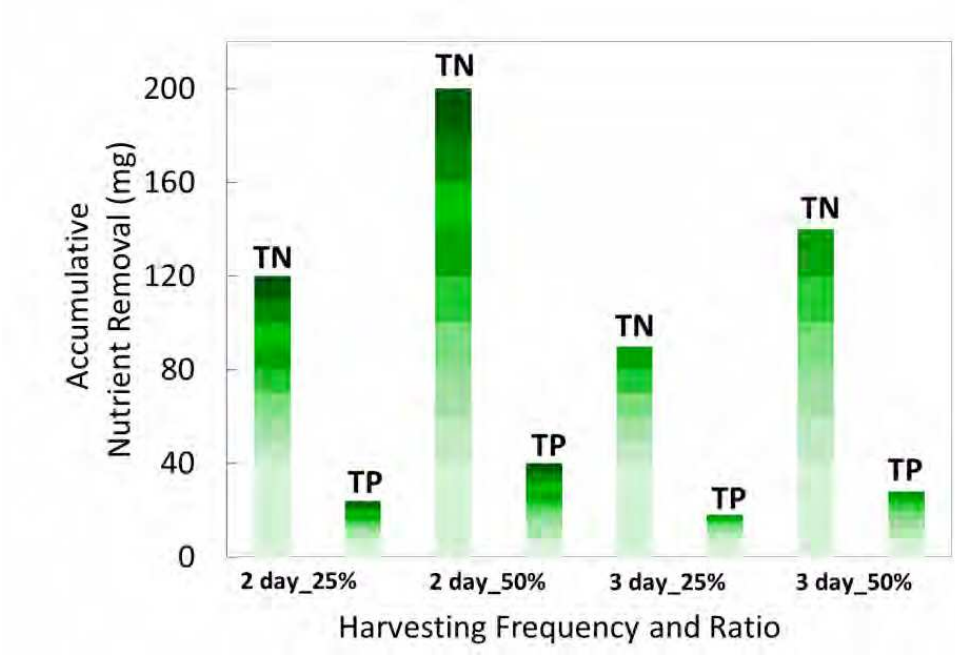

Figure 21. Accumulative nutrient removal at different conditions during an 18-day semi-continuous experiment

The accumulative algae biomass production was highest when 50% of algae were harvested and AD effluent was replenished every 3 days. The highest accumulative nutrient removal was obtained when 50% of algae were harvested and AD effluent was replenished every 2 days.

Nannochloropsis is a genus of yellow green algae of the family Monodopsidaceae that is less than 5 μm in its maximum dimension (Hibberd, 1981). Members of this genus include 6 species: *N. gaditana, N. granulate, N. limnetica, N. oceanica, N. oculata, N. salina* (Andersen et al., 1998; Hibberd, 1981). Among these various species, *N. salina* is attractive because it is marine algae and has a relatively high biomass and lipid productivity (Boussiba et al., 1987; Emdadi and Berland, 1989). Therefore, it is a promising candidate for biofuel production. Additionally, *N. salina* is mixotrophic, which means that it cannot only uptake the organic carbon in the anaerobic digestion effluent but also perform photosynthesis to sequence carbon oxide in the air or flue gas (Gonen-Zurgil et al., 1996; Huerlimann et al., 2010; Zittelli et al., 1999).

Seed culture and filtrate of anaerobic digestion effluent

Seed culture of *Nannochloropsis salina* was provided to OARDC for the studies from Touchstone at approximately 2% salinity and pH approximately 8.5. Effluent was collected from a commercial-scale wet anaerobic digester from quasar energy group (Wooster, OH). The effluent was filtered using a 10000 molecular weight cutoff Sepa™ crossflow polyethersulfone ultrafiltration membrane (GE Osmonics, Minnetonka, MN), which was mounted on a Sepa™ CF II membrane cell system (GE Osmonics, Minnetonka, MN). The operating pressure of the membrane was maintained at 689 kPa (100 psi), and the operating temperature was kept at 21°C.

Using an inductively coupled plasma mass spectrometer model 7500cx (Agilent Technologies, Santa Clara, CA), both materials were analyzed for the concentration of 13 various elements – sodium (Na), magnesium (Mg), aluminum (Al), phosphorus (P), potassium (K), calcium (Ca), iron (Fe), manganese (Mn), nickel (Ni), cobalt (Co), copper (Cu), zinc (Zn), and molybdenum (Mo). **Table 5** shows the concentrations of all detectable elements in the algae seed culture and effluent ultrafiltrate.

Table 5. Detected nutrient concentrations found in materials for algae growth by ICP-MS.

Sample	^{23}Na (μg/g)	^{24}Mg (μg/g)	^{31}P (μg/g)	^{29}K (μg/g)	^{44}Ca (μg/g)
Algae seed from TRL (3/15)	7292	810	0	250	22
AD effluent ultrafiltrate	2042	0	829	891	0

Batch culture of N. salina

Each reactor consisted of a 2 L glass bottle capped with a rubber stopper. The air inlet for the reactor was made with stainless steel tubing with a 4.76 mm (0.1875 in) inner diameter (ID). A polypropylene tee barb was connected at the bottom of the reactor to evenly disperse the incoming air in a horizontal direction and prevent algae from adhering to the reactor wall. The light chamber was enclosed with white coated metal walls to maintain the photobioreactors at a constant temperature of 25°C. One 32 W GE F32T8-SPX50 fluorescent lamp (GE Lighting, Ravenna, OH) was used for up to six reactors to provide a constant photosynthetic photon flux of approximately 200 μmol m^{-2} s^{-1}, measured by a BQM quantum meter (Apogee Instruments,

Logan, UT). Air was provided under 27.6 kPa (4.0 psi) to a custom-made polyvinyl chloride (PVC) gas manifold, which provided a constant air flow of 500 mL/min to each reactor through clear PVC tubing. The salinity of each reactor was adjusted to 2%.

Analytical Procedures

Among the numerous peaks in the absorption coefficient spectrum of *N. salina*, two distinct maxima exist at approximately 440 nm and 680 nm. The peak near 440 nm represents the chlorophyll-a concentration at the Soret region (Gitelson et al., 2000). The optical density peak at 440 nm was used to establish a relationship with cell concentration. A Biomate 3 spectrophotometer (Thermo Fisher Scientific, Madison, WI) was used to measure the absorbance of cells at 440 nm.

Algal biomass was represented by its ash-free dry weight (AFDW), which was determined gravimetrically. Fifty grams or similarly measured sample was placed in a clean centrifuge tube and centrifuged at 10,000 rpm for 15min. The supernatant was used for measurement of nutrients removal rates. The precipitate was washed with 25 ml 0.5 M NH_4HCO_3 solution and then centrifuged at 10,000 rpm for 15 min. The precipitate was washed again with 10 ml 0.5 M NH_4HCO_3 and transferred to a clean, ignited, and tared porcelain crucible and dried in a Thelco Model 18 oven (Precision Scientific, Chennai, India) at 95°C for 12 hours. After the sample was brought to constant weight, it was cooled in a desiccator and weighed. Ash weight was obtained by igniting the sample in an Isotemp muffle furnace (Fisher Scientific, Dubuque, IA) at 500°C for four hours. The AFDW was calculated to be the difference between the dry weight and the weight of the ash residue after ashing.

Inductively coupled plasma-mass spectrometry (ICP-MS) was used to assess the concentration of 13 various elements – Na, Mg, Al, P, K, Ca, Fe, Mn, Ni, Co, Cu, Zn, and Mo – in the effluent filtrate, algae seed, and biomass filtrate. An ICP-MS unit 7500cx (Agilent Technologies, Santa Clara, CA) was used along with US EPA method 6062A. Prior to ICP-MS analysis, the sample was digested in a Microwave Accelerated Reaction System (CEM Corporation, Matthews, NC) at 190°C for 10 minutes. The digested sample was diluted 50-fold and analyzed via ICP-MS. The nitrogen removal was determined by measuring the total nitrogen contents in the effluent filtrate, algae seed, and biomass centrifuge supernatant. The centrifuge supernatant indicating the nitrogen content in the culture medium alone was obtained with a Sorvall Legend T+ centrifuge (Thermo Scientific, Osterode, Germany) operated at 10000 rpm for 10 minutes. A Vario MAX CNS elemental analyzer (Elementar Analyseneyeteme GmbH, Hanau, Germany) was used to determine the mass proportion of nitrogen in all samples.

Ultrafiltration of effluent

Ultrafiltration was used to remove the microorganisms and particles in the AD effluent before feeding the effluent to algae as a nutrient source. As shown in **Figure 22**, the turbidity of the permeate is much lower than that of the initial effluent, and it is beneficial for microalgae to have high photosynthesis efficiency. After ultrafiltration, the total volume recovery rate of the permeate is 84%. The recovery rates of TKN, NH3_N and Phosphorus are 62%, 74% and 78% respectively as shown in **Figure 23**.

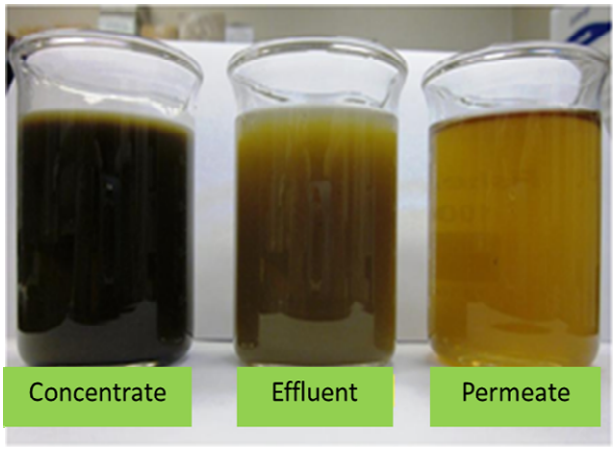

Figure 22. Turbidity contract between NH3, effluent, and ultrafiltered permeate

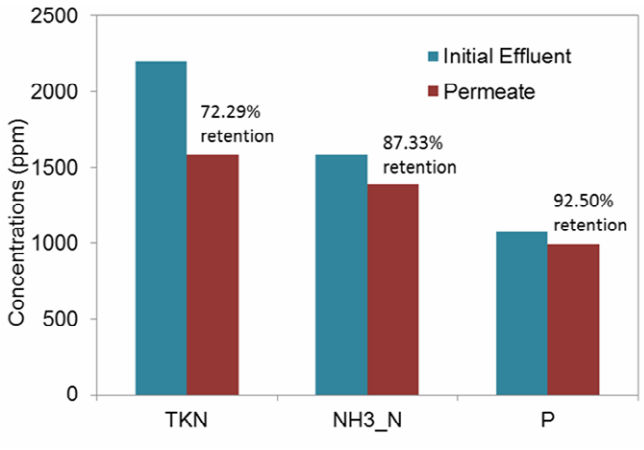

Figure 23. TKN (total Kjeldahl nitrogen) and phosphorus contents of the effluent and ultrafiltered permeate

Effect of permeate loading on algae growth curve and biomass yield

Optical density (OD) of the algae culture was used as a parameter to monitor algae growth. **Figure 24** shows the algae growth curve fed with different concentrations of permeate. There was no obvious lag phase observed with 5% permeate loading (27ppm TN). Higher effluent loading rate inhibited algae growth at the beginning. The growth rate in 5% (27ppm TN) level is not the highest among the five levels. However, considering nutrient recovery efficiency, 5% (27ppm TN) should be the most appropriate effluent feeding level for continuous algae culture.

The correlation between biomass yield and OD value is good (R^2 = 0.9894), which means that OD value is a proper indicator for algae growth (see **Figures 25 and 26)**.

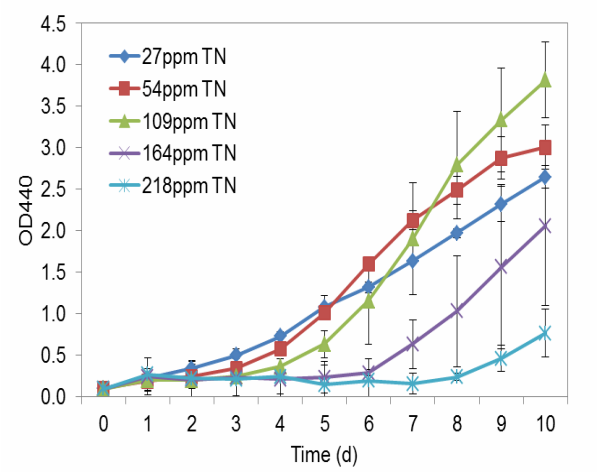

Figure 24. Effect of effluent concentration on OD

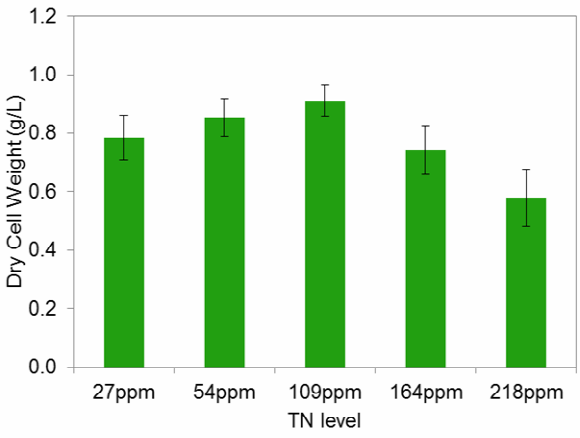

Figure 25. Effect of effluent concentration on biomass yield

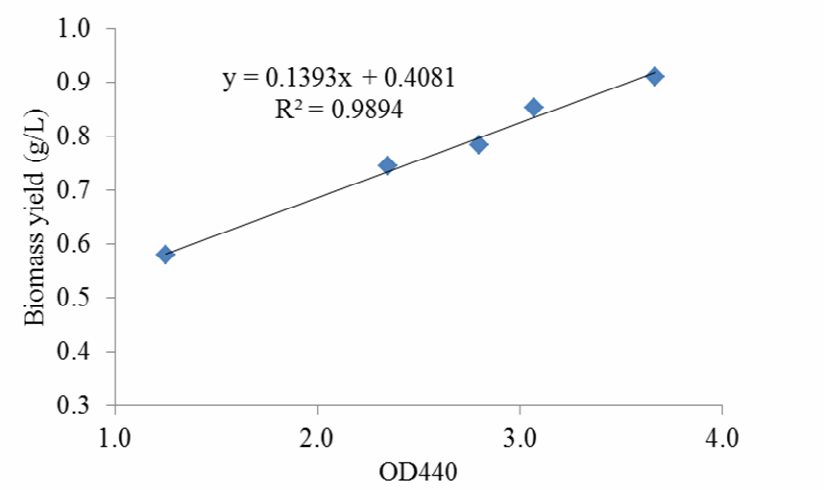

Figure 26. The correlation between biomass yield and OD value

Effect of inoculum size on algae growth cure and biomass yield

The specific growth rate of algae increased remarkably as the inoculum size increased from 0.02g/L to 0.08g/L (**Figure 27**). Starting from 0.12g/L, the growth rate remained the same or decreased because of the self-shading effect and nutrient competition. The 0.08g/L inoculum size also gave highest final OD value and biomass yield, which makes it the optimal inoculum size for semi-continuous culture (see **Figure 28**).

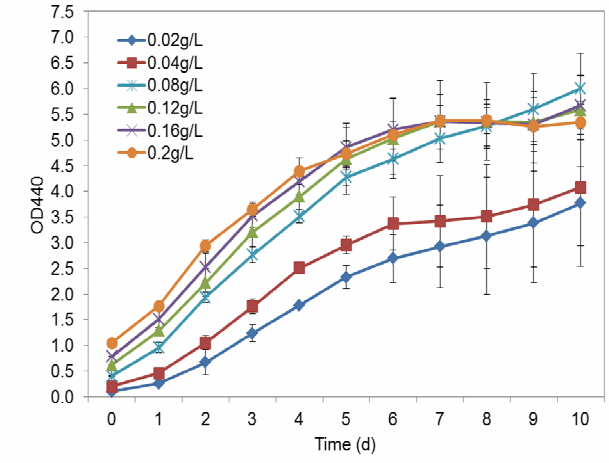

Figure 27. Effect of inoculum size on OD

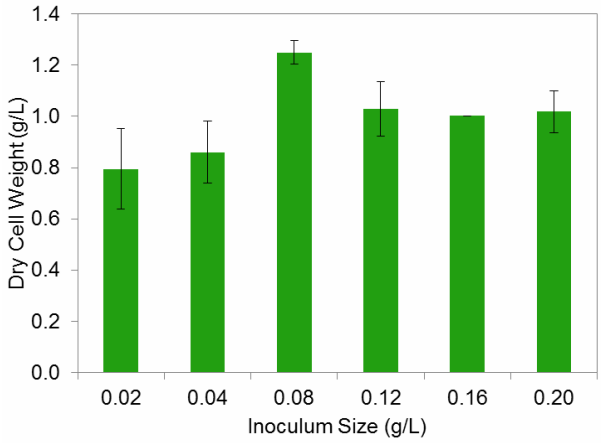

Figure 28. Effect of inoculum size on biomass yield

OARDC investigated a microfiltration separation system and a separation system utilizing a centrifuge. Based on previously reported work between the microfiltration system and a commercial centrifuge system, the AD effluent was prepared utilizing a commercial centrifuge from an existing AD system.

3.3 Extraction and Conversion Technologies

Lipid extraction and characterization tests on algae biomass provided by Touchstone were performed by SRS. Additional bench-scale trials were also conducted to optimize the SRS extraction process for the algae biomass.

Extraction methodology: In exploring for the best extraction method, SRS tested the Algae Frac™ extraction system, which employs modified solvent extraction of aqueous algae paste. These methods have the benefit of allowing direct extraction of lipid from a wet sample; however, the goal is to be able to process large quantities of algae in a cost-effective and environmentally friendly way, and, thus, investigation eventually led to a solvent-based extraction method that utilized hexane and propane as the extraction solvents. Algae Frac™ extraction involves refluxing a solvent to repeatedly wash and extract the sample; then the lipid is obtained by evaporating off the solvent. The benefits of using this extraction method include: (1) the extraction solvent (hexane/propane) can be recycled and reused, (2) propane is easier to handle than the hexane and, thus, more environmentally friendly, and (3) the lipids obtained with this extraction method are neutral lipids that are ready for conversion into biofuel.

Lipid extraction

1) **Bench scale process:** For Algae Frac™ extraction samples tested (**Figure 29**), approximately 300 grams of wet algae paste were placed in an extraction chamber and pre-treated. The extracted lipids and algal paste were transferred to a two-liter separation flask to retrieve the solvent fraction. The solvent fraction was transferred to a round bottom flask in a rotary evaporator unit. This process was followed by attaching a water bath to the top of the extractor with cold water running through to help condense the rising solvent vapor. Lastly, heat was applied and the extraction was allowed to run until the solvent was removed completely.

Figure 29. A photograph of extracted algae oil using different conditions

2) **Large-scale/Pilot-plant process:** Two larger fractionation batches were carried out to process approximately 20 Liters of algae paste in each batch. A number of bench trials were planned and carried out to identify the most optimum process parameters for large batch processing. Requisite pilot modifications were carried out, and the two batches of

20L algae paste were processed. The process ran very efficiently and did not have any significant processing issues. The oil/solvent mixture was portioned and distilled to produce approximately 830 grams of crude algae oil in each batch, with an extraction yield of 35% w/w AFDW. This crude algae oil was used to perform experiments for fuel conversion and up-grading. Spent algae biomass was recovered and was sent to OARDC for evaluation as a feedstock for anaerobic digestion.

Lipid characterization

The main aim of the lipid characterization was to identify and quantify the fatty acid methyl esters (FAMES) derived from mono, di- and tri-acylglycerides. An approximate identification by alkyl chain length can be made using the retention times compared to standards by chromatographic analysis using GC with a FID and HPLC coupled Evaporative Light Scattering Detector (**ELSD**) system. A more precise identification is obtained using the GC-MS. In the first step, triacylglycerides (TAGs) are extracted from a wet sample using the Algae Frac^{TM} method. In the second step, the extracted TAGs are transesterified to FAMES. The FAMES are dissolved in a known quantity of heptane and then analyzed by GC-FID.

For analyzing the samples through GC-FID, a calibration curve was made using a known concentration of external standards of fatty acid methyl esters (FAMES) and their chromatographic peak areas. This calibration curve was helpful to:

(i) Identify peaks in the unknown sample run using the same GC-FID method as used for standards.
(ii) Develop a standard linear curve for the known standards which could be used for calculating the concentration of the unknown peak eluting at the same retention time as the standard peak.

The concentration of the peak eluting between the retention times of more than two known standard peaks was calculated by taking an average of the concentrations obtained by using the standard curve of the neighboring standard peaks. The standards used for this analysis included: Lauric acid methyl ester (C12:0), Myristic acid methyl ester (C14:0), Myristoleic acid methyl ester (C14:1), Palmitic acid methyl ester (C16:0), Palmitoleic acid methyl ester (C16:1), Stearic acid methyl ester (C18:0), Oleic acid methyl ester (C18:1n9c), Elaidic acid methyl ester (C18:1n9t), Linoleic acid methyl ester (C18:2n6c), Linolelaidic acid methyl ester (C18:2n6t), g-Linolenic acid methyl ester (C18:3n6), Linolenic acid methyl ester (C18:3n3), Arachidic acid methyl ester (C20:0), cis-11-Eicosenoic acid methyl ester (C20:1), cis-11,14-Eicosadienoic acid methyl ester (C20:2), cis-8,11,14-Eicosatrienoic acid methyl ester (C20:3n6), Heneicosanoic acid methyl ester (C21:0), cis-11,14,17-Eicosatrienoic acid methyl ester (C20:3n3), Arachidonic acid methyl ester (C20:4n6), cis-5,8,11,14,17-Eicosapentaenoicacid methyl ester(C20:5n3), Behenic acid methyl ester (C22:0), Erucic acid methyl ester (C22:1n9), cis-13,16-Docosadienoic acid methyl ester (C22:2), Lignoceric acid methyl ester (C24:0), cis-4,7,10,13,16,19-Docosahexaenoic acid methyl ester (C22:6n3)

Sample preparation for GC analysis

Approximately 100 mg of algal lipid was added to a small Teflon-capped vial (40mL) with 10 mL methanol in it. Next, 0.8 mL of 5% acetyl chloride in methanol was added to the vial. The vial was tightly capped and heated in a water bath at 120^{o}C for 1 hour. After cooling, the sample was adjusted to ~10000 ppm concentration with heptane. The heptane was taken up in ~2 mL of HPLC vial and analyzed by GC-FID (Flame Ionization Detector). **Figures 30** and **31** show typical fatty acid profiles of the samples listed in **Appendix A**.

Gas chromatography mass spectrometry (GC-MS) analysis

The gas chromatograph electron impact mass spectrometer is a powerful and extremely useful instrument that combines two techniques to allow a single method of analyzing mixtures of fatty acids. Through gas chromatography, the components of a mixture were first separated; subsequently, the separated components were characterized and identified individually by mass spectrometry.

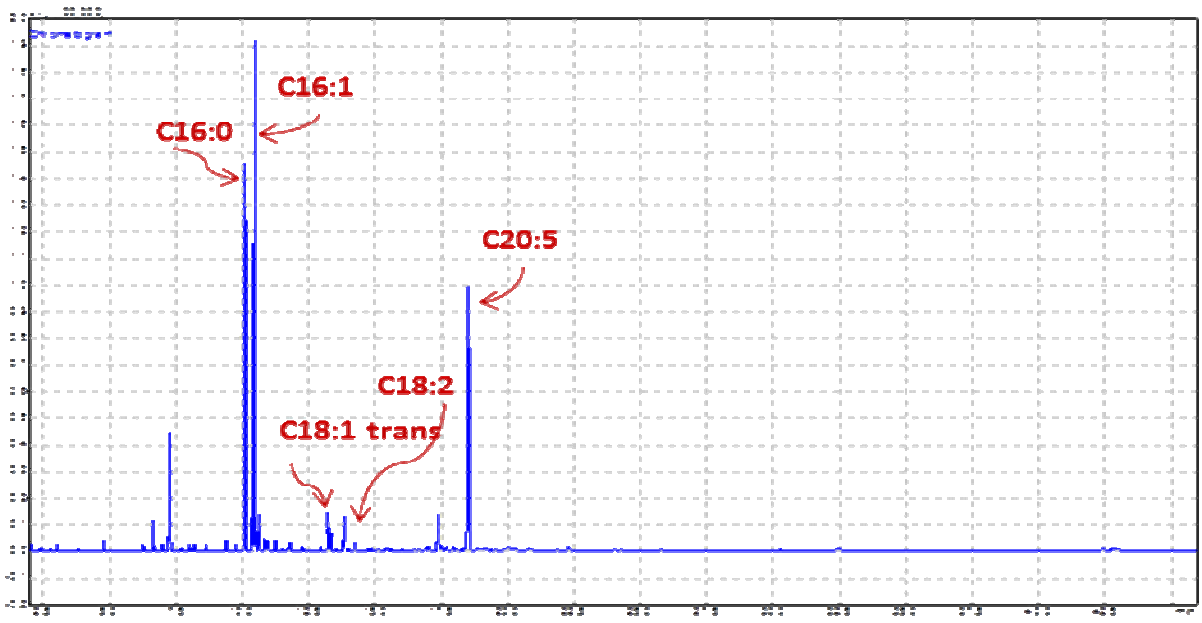

Figure 30. Lipid profile of *Nannochloropsis salina* separated and identified by GC-FID

By combining these two techniques, GC-MS analysis not only allows qualitative and quantitative evaluation, but also identification of fatty acids in a mixture solution. Pertinent to this project, this instrument allows efficient identification of specific fatty acids contained in the various extraction runs of algae oil. In the future, this instrument will aid in qualitative and quantitative evaluation of the different chain length FAMEs in the biofuel produced from the algae oil. The total glycerides and free fatty acids content of the algae species were determined using the GC-FID, GC-MS and HPLC coupled ELSD system.

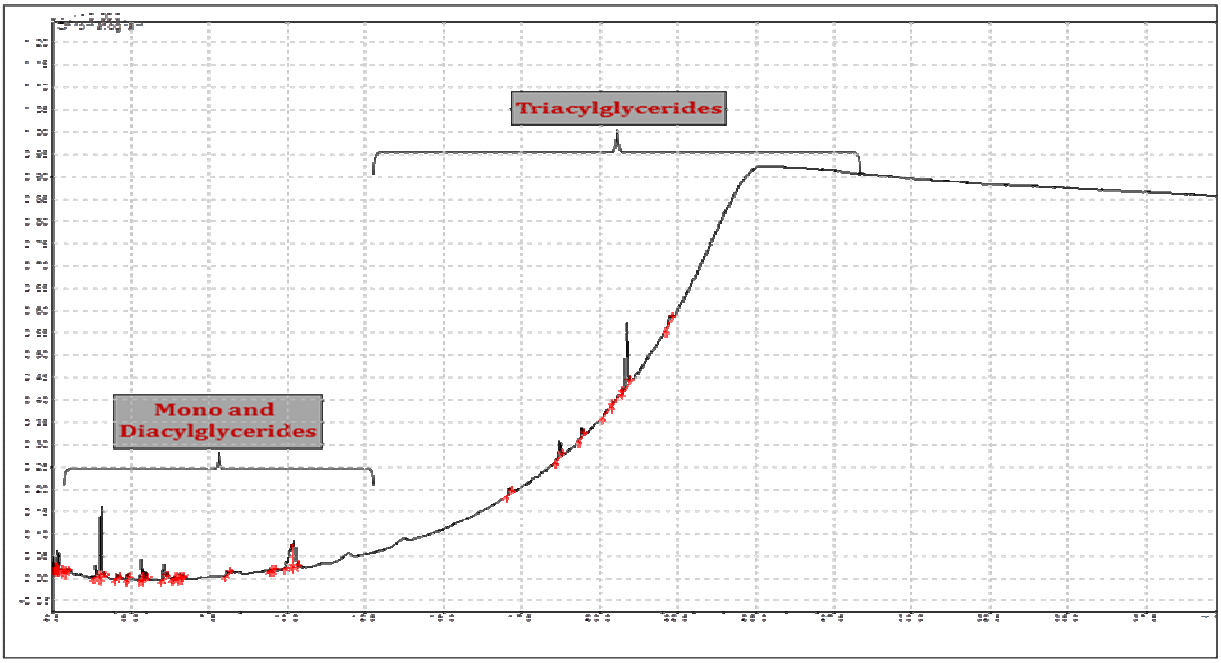

Figure 31. Sample chromatogram showing GC-FID spectrum of *Nannochloropsis salina* mono, di and triacylglycerides separation and distributions

Lipid extraction using propane and triacylglycerides separation and quantifications were in progress. Also, experiments had been conducted to identify the optimum operating conditions and to investigate the possibility of production of other value-added co-products.

A distillation process primarily used to concentrate omega-3 fatty acids (EPA and other value added products) in algae oil and to remove other bio-molecular contaminants was developed. **Figure 32** shows the fractionation temperatures and amounts collected for a representative experimental batch.

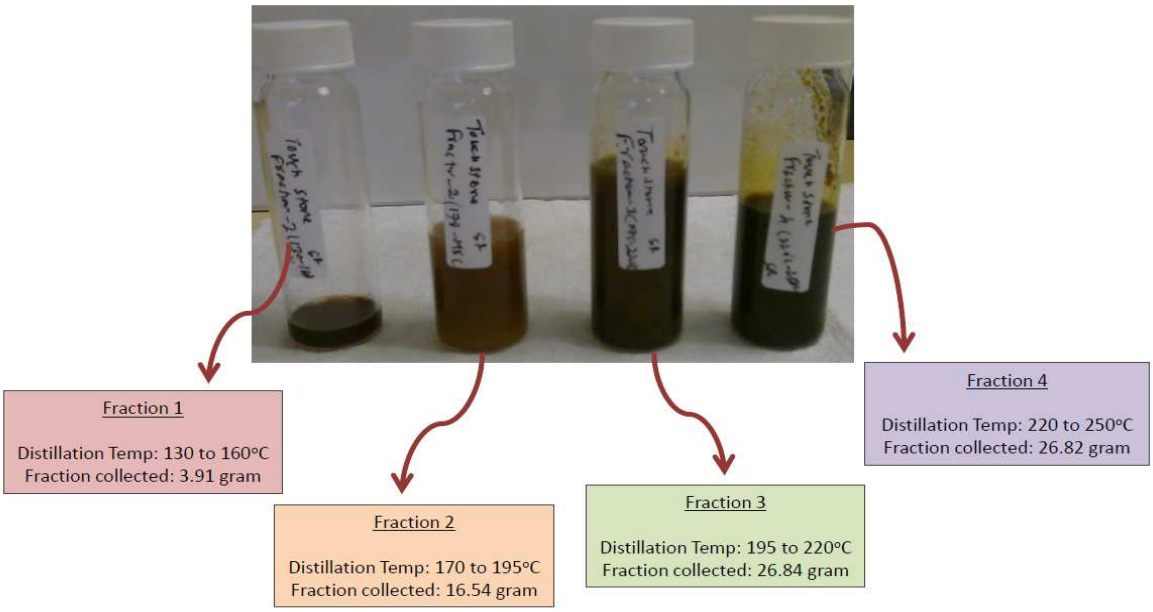

Figure 32. Distribution of distillation temperature of the fractions from vacuum distillation of Touchstone algae oil

Further distillation process development involved:

- Converting the algae oil into a methyl ester and fractionating the methyl esters and fatty acids from crude oil in a vacuum system with elevated temperatures.
- Utilizing high throughput Wiped Film Evaporators and Molecular Distillation approaches to isolate and enrich the esters and fatty acids.

A larger-scale extraction was carried out on one approximately 8 kg batch of harvested algae concentrate from the ongoing raceway studies underway at Cedar Lane Farms. As reported by SRS, the extraction process was conducted very efficiently and did not have any significant processing issues. The crude algae oil/solvent mixture was separated during the processing and distilled to produce 431 grams of crude algae oil, with a corresponding extraction yield of 65.97% w/w AFDW. The spent biomass was recovered and sent to Dr. Yebo Li, OARDC.

3.4 Pilot Plant Design and Construction

An algae pond complex was designed and built as a pilot plant for continuing algae biofuel research. The pilot plant consisted of a multiple-pond arrangement providing a lagoon capacity of one acre (nominal). The 1-acre capacity represented a nominal algae recovery capacity of 50 tons per year (dry basis). The 50-tpy algae recovery rate equates to the following: minimum annual capture rate of 60%, minimum yield of algae-based organic lipids of 25% by weight, equivalent recovery of 3290 gallons of algal oil that represents a bio-crude fuel intermediate product that can be refined to the fuel forms of biodiesel oil (2185 gpd) and bio-bunker oil (1390 gpd), anaerobic digestion of the algae residue and recovery of 731,250 ft^3 per year of biogas at an equivalent fuel heating value of 600 Btu/ft^3 and equivalent fuel heat input of 50 kBtu/hr, and the byproduction of 5 kW of electrical power through IC engine generation operating at a nominal heat rate of 10,000 Btu/net kWh.

The four raceway lagoons represented the centerpiece of the process where CO_2 was converted to algae. Each pond consisted of a raceway lagoon design that circulated flow counterclockwise around a center island propelled by paddlewheels. The common elements of each were aqueous solution (saline water solution at 20 ppt salinity), dimensions (48-ft by 189-ft oval with a 2-ft center island), capacity (50,914 gallons of underlying algae liquor topped by 7637 gal of PCM), mixing sump (4-ft sump complete with baffles, fine bubble diffuser, double paddle wheel, and algae harvesting pump), aquatic instrument packages and sampling ports (4 and 8 locations each), and pond liner (HDPE material). Four ponds provided the experimental design: two were equipped with PCM and two without, two with cover and two exposed (2x2 experimental control matrix).

The proposed process flow proceeded stepwise per the following description: A slip stream of flue gas was taken from the AFBC downstream of the existing fabric filter's discharge point, thus providing a flue gas stream that was well controlled for PM, SO_2, NO_X, CO, HCl, Hg, and particulate-phase trace element HAPs. Only one-fiftieth ($^{1}/_{50}$) of the unit's flue stream (66 acfm/44 scfm) was needed to provide sufficient CO_2 to meet the algae recovery target. The flue gas slip-stream was to be quenched (partially quenched to a temperature of 180°F to both attemperate and condition the gas stream prior to pond injection), boosted via a booster fan, and then injected into the ponds via a fine-bubble diffuser installed at the sump base of each pond. Algae was to be harvested from each pond as a dilute solution (< 0.5% solids by weight), concentrated via primary dewatering (centrifuge or diffused air flotation). The concentrated algae product (12% solids) was to be shipped off-site as an off-take for recovery of algal oil (bio-crude) via physical (filter press) or solvent (hexane) extraction of the chemical lipids. Liquor was to be returned to the process (262 gph) and balanced with fresh makeup water (10 gph). The off-site off-take streams included algal oil that was to be recovered as a bio-crude fuel form (0.4 gph), which was to be refined to biodiesel fuel (0.3 gph) and bio-bunker fuel (0.2 gph) forms, biogas from anaerobic digestion of algae residue (85 scfh), and power generation via combustion of the biogas in an IC engine generator (5 kW). Balance-of-plant (BOP) operations included tankage and feed pumps for inoculant storage and feed, PCM storage-cleaning-recirculation, and water-liquor storage and surge. Support operations included the auxiliary combustor (aux combustor), flue gas cooler, and flue gas storage. **Figure 33** shows the finished indoor ponds, and **Figure 34** shows the finished outdoor ponds.

Figure 33. Indoor ponds

Figure 34. Outdoor ponds

Figures 35 and 36 show pictures of the auxiliary items that were needed for algae production.

Figure 35. Processing area and inoculation tanks

Figure 36. Algae harvesting area and laboratory building

OpenAlgae was brought in to provide a pilot extraction system for on-site harvesting and lipid extraction. The OpenAlgae system provided for harvesting of about 20,000 gallons per day. The concentration unit utilized pH flocculation to concentrate the algae. The extraction system utilized electromechanical pulses to lyse the algae and, subsequently, separate the lipid material utilizing a membrane separation system. Based on harvesting activities with OpenAlgae's existing equipment, some changes were made to the design of the concentration unit. These changes created a slight delay in the delivery of the concentration unit, but while the system was under construction, OpenAlgae provided existing equipment on site for harvesting.

The Open Algae electromechanical cell lysing unit was installed on May 13, 2013 (see **Figures 37 & 38**). An initial verification of system functions was performed May 14-15, 2013. The cell lysing unit can create an electric field of up to 18 kV/cm and pulse durations from about 5 μs to about 30 μs. Previous work on fresh water algae indicated 8 KV/cm and 15 μs is sufficient to lyse most fresh water algae.

Figure 37. Algae lysing unit control system

Figure 38. Lysing chamber

The algae lysing unit had two pulsing chambers. The pulsing chambers were indicated by the orange insulators in the above photo. Concentrated algae was pumped from the bottom to the top, exposing algae to the electromechanical pulses as the algae concentrate flows through each of the two reaction chambers.

An initial verification of system functions was performed, and the performance was found to be acceptable. The algae oil recovery unit (**Figure 39**) was designed to separate non-polar lipids from lysed algae biomass. By separating the non-polar lipids from polar material such as phospholipids and nitrogen-containing materials, the oil recovery was anticipated to supply a direct biofuel intermediate for biofuel conversion. The biofuels intermediate was to be substantially free of catalyst-poisoning phosphorous and nitrogen-containing compounds.

Figure 39. Oil recovery unit, (L) front view and (R) back view

The oil recovery unit had two membrane cartridges: a large membrane cartridge for processing large volumes of material (shown in **Figure 40**) and a small cartridge for processing smaller volumes.

Figure 40. Membrane cartridge

Based on previously reported work, between the microfiltration system and a commercial centrifuge system the AD effluent was prepared utilizing a commercial centrifuge from an existing AD system (**Figure 41**).

Figure 41. The ANDRITZ centrifuge system, which is used to prepare the AD effluent for algae cultivation

3.5 Pilot Plant Operation

Construction and shakedown of the pilot facility was completed during the first two years, and the focus of the last year was on operations and the cultivation of algae. Continuous harvesting activities yielded over 200 kg algae dry weight for ponds 1, 2 and 4. Studies were conducted to determine the effect of anaerobic digestion effluent as a nutrient source and the resulting lipid productivity of the algae. Lipid content and total fatty acids were unaffected by culture system and nutrient source, indicating that open raceway ponds fed diluted anaerobic digestion effluent can obtain similar lipid productivities to open raceway ponds using commercial nutrients.

The following major system components were tested:

- Ponds – Each pond was cleaned, filled with water, and leak checked to a height of 20-22 inches.
- Pipe Storage – Pipe storage of major piping component was determined.
- Facility Mechanics – Pumping and flow rate verification to and from all major processing areas.
- Water Quality Sensors – Water quality probes and sensors were calibrated for each pond.
- Data Collection – Data collection from water quality sensors to the central computer was established.
- Gas Analyzer Calibration – The gas analyzer was set up and calibrated utilizing standard calibration gases.
- Paddlewheel Calibration – Paddlewheel function was verified. Paddlewheel speed was calibrated to provide sufficient water flow rate.
- Inoculation System Testing and Start Up – Inoculation tanks, piping, and pump functions were verified. Began initial inoculation of 200 gallon vertical tanks.
- Gas Stream Capture and Controls – Gas diffusers were positioned in ponds. Verified control of flue gas flow rates. Established and verified collection of flue gas composition and flow rate data. Problems existed with the high levels of water generated in the flue

gas stream. These high water levels were damaging flow meters and gas monitoring equipment. The addition of spray nozzles and a water drop-out drum installed before the flow controllers and gas analyzer reduced the condensation in the flue gas line dramatically such that the system is now operational.

- Harvest Flow Rates – Tested harvest pumps and flow rates.

Algae cultivation activities began with the inoculation of Pond 4 (greenhouse control pond). The pond was initially inoculated with 1.4 kg of algae on June 15, 2012. Initial growth was monitored by UV-vis spectroscopy (440 nm), and contaminants were monitored by microscopy. As shown in **Figure 42**, initial growth was strong for the first five days. Contaminants were observed on day 6, and a decrease in algae density was detected. By day 8, the contaminant population decreased, corresponding with an increase in algal growth for the next week. Depending upon the growth rate and condition of Pond 4, the other ponds could have been inoculated using Pond 4.

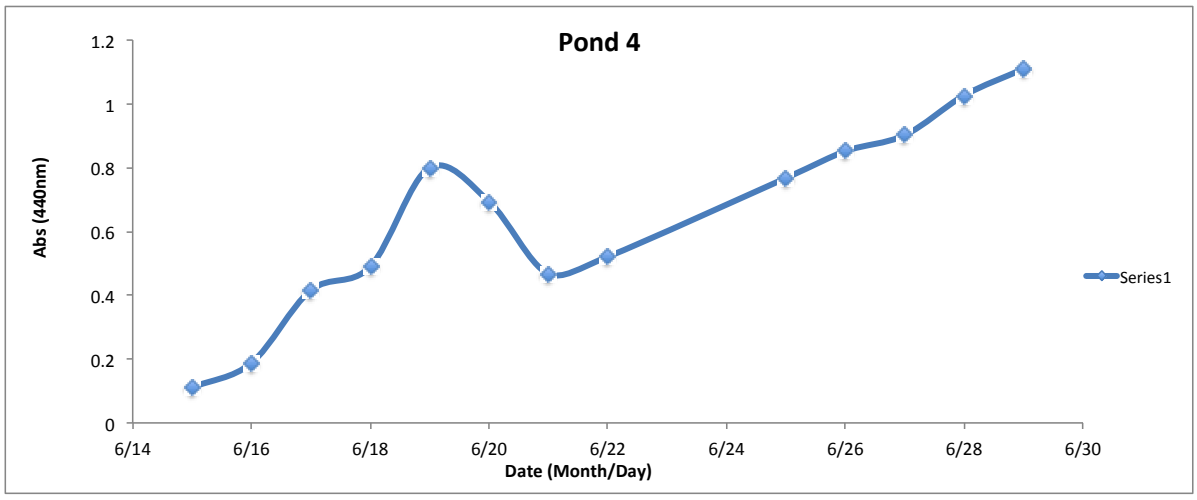

Figure 42. Plot of absorbance as a function of time for Pond 4

All four pilot-scale raceway ponds were inoculated, and growth was monitored by UV-vis spectroscopy (440 nm) as well as by dry weight measurements. PCM material was added to Pond 3 (indoor PCM pond). Contaminants were monitored by microscopy. Ponds 1, 2, and 4 (without PCM) were each able to reach about 0.6 grams algae/liter dry weight (DW) and were able to maintain a relatively stable concentration over about two weeks before declining. The concentration in Pond 3 with the PCM material did not go above 0.4 grams algae/liter DW. An interesting observation with respect to Pond 3 was the consumption of nitrogen and phosphorous nutrients. While algae concentration measurements from Pond 3 were typically low, Pond 3 consumed at least twice the quantity of nitrogen and phosphorous.

PCM Emulsion Formation+

An emulsion began forming on the surface of Pond 3, and after a few days the entire surface of the pond was covered with an emulsion. The installed baffle system could not prevent the PCM material from being drawn into the paddlewheel region, and its recycling system through the baffle and pump appeared to create much of the emulsion. Additionally, the mixing of the PCM material in the paddlewheel region contributed to the formation of an emulsion layer between the water and the PCM material. To reduce the formation of this layer, the paddlewheels were replaced with underwater screw pumps for circulating water. In this way, the interface between the PCM layer and the water layer were not be disrupted as severely as with the paddlewheel, and the baffle system was removed entirely to reduce the possibility of the formation of an emulsion.

The initial configuration of the screw pumps had the auger perpendicular to the length of the pond. Several challenges were created with this configuration and materials. The horizontal orientation of the auger was not efficient, the casing material was too flexible, and the water intake needed to be lowered such that no surface water or PCM material would be drawn into the pumps (see **Figure 43**).

Figure 43. Screw pumps installed in Pond 3

The screw pumps as installed needed modifications to prevent the PCM material from entering the pumps. As seen **Figure 44**, the intake pipe from the screw pump has a tendency to float, and the intake for the screw pump pulls in water and PCM material. The pumps were redesigned such that the pipes did not float and the intake for the pump was positioned well below the surface of the water.

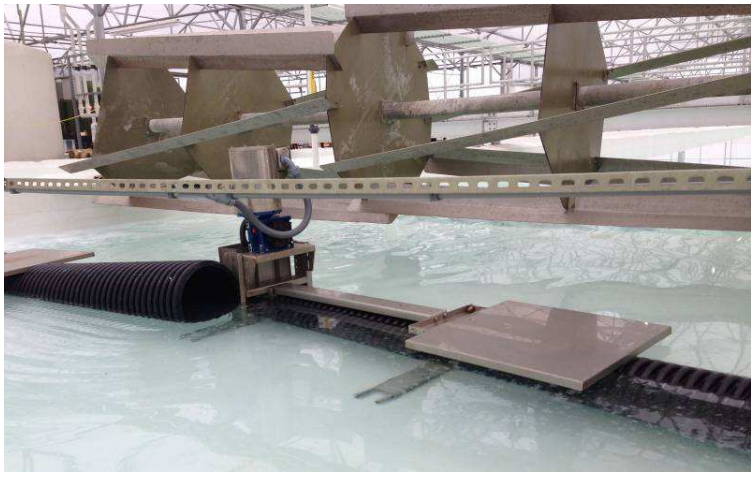

Figure 44. Intake pipe floating to surface

The water movers were modified as shown in **Figures 45 and 46**. The water intakes were lowered. The auger was positioned at about a 60 degree angle with the water flow, and the auger was encased in rigid polymer pipe.

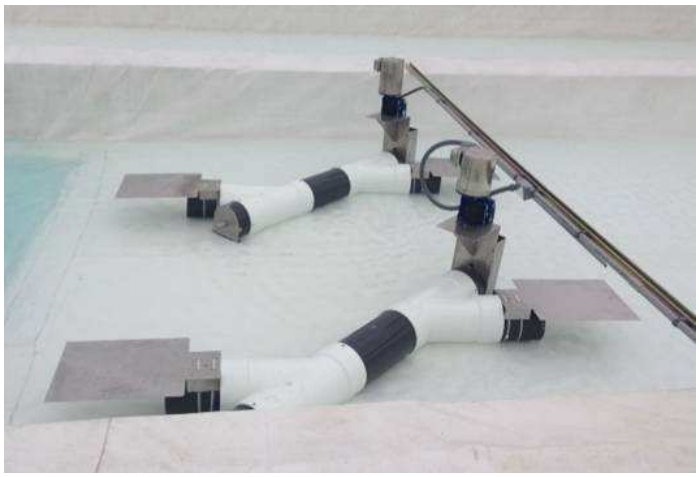

Figure 45. Redesigned water movers

While this design was much more effective, flow rates dropped significantly after 5-7 days. The belt that drove the pumps would become slippery, presumably due to algae, and lose grip on the drive wheel. To use this configuration in the future, a belt with a sprocket system would need to be utilized.

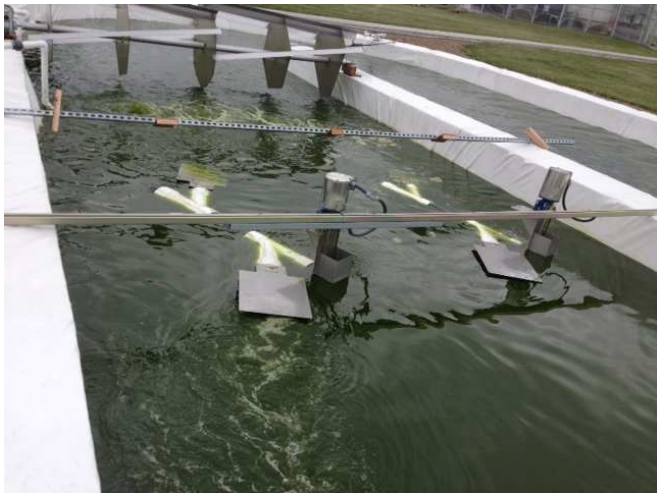

Figure 46. Redesigned water movers in operation

Ultimately, the paddlewheel was used at a reduced rate without the underwater screw pumps. Reducing the rpm of the paddlewheel to keep the flow above about 0.5 ft/sec kept the emulsion from forming on the surface of the pond. While the flow rate was lower than desired, it was determined to be a reasonable trade-off to minimize a surface emulsion from forming on the surface of the pond.

Evaporative Water Loss

Ponds 3 and 4 (greenhouse ponds) were monitored for evaporative water loss from August 14 – August 31. During this time period, Pond 4 with no PCM material averaged 357 gallons of water loss/day. Pond 3 with the PCM layer averaged 214 gallons of water loss/day. The thin layer of PCM material provided about a 40% reduction in evaporative water loss. Most of this water loss is thought to have occurred around the baffles and paddlewheel area.

Water loss for Ponds 1 and 2 (outdoor ponds) was monitored. Pond 2 (PCM pond) had no baffles and was using the paddlewheel to achieve a reduced flow rate of about 0.5 ft/sec. The layer of PCM material was less than 1/8 of an inch, and the entire surface of the pond was covered with PCM except for minor disruption areas due to the paddlewheel and exposed areas when the PCM would solidify and change phases.

The small amount of PCM material on Pond 2 significantly reduced water loss when compared to the control pond. From September 10 – October 1, after factoring in water accumulation due to 2.4" of rainfall, harvesting activities, and water additions to keep the pond levels above 8.5" in total depth, Pond 2 (PCM pond) lost 15,505 liters of water compared to 59,565 liters of water for Pond 1 (control pond), resulting in a 74% reduction in water loss for the PCM pond.

Alkalinity

The harvesting of algae using a pH flocculation technique requires an increase in pH to about a pH of 10 to flocculate the algae. At this point the flocculated algae may be separated creating an algae "concentrate" and "effluent." Before the effluent is returned to the pond, the pH of the effluent is lowered to around a pH of 7. As will be discussed below, depending upon how the

pH is controlled during harvest, an increase in alkalinity can occur in the pond resulting in an increase in material consumption and costs.

For example, during the processing of Pond 4, the alkalinity of Pond 4 increased from an initial alkalinity of 380 ppm (2-14-13) to over 1440 ppm (5-2-13). This increase in alkalinity led to increased NaOH usage for the algae concentration unit. The increase in alkalinity was attributed to how the pH was controlled during the harvesting operation.

The algae concentration unit raised the pH of the pond water to 10.2 through the addition of NaOH. Before the water was returned to the pond, the pH was lowered to 7.5 by introducing CO_2. While CO_2 is a convenient way to lower the pH, the net result of this process is the build-up or blow-down of sodium bicarbonate to the pond. As the alkalinity increases, the buffering capacity of the pond increases resulting in increased NaOH usage during harvesting.

To raise pH to pH 10.2 (equations not balanced):

$$H_2O + NaOH \rightarrow H_2O + Na^+ + OH^-$$

Lowering pH with CO_2 to 7.5:

$$\text{(pH 10.2) } CO_2 + H_2O \rightarrow 2H^+ + CO_3^{2-}$$

$$H_2O + Na^+ + OH^- + 2H^+ + CO_3^{2-} \rightarrow \mathbf{H_2O + Na^+ + CO_3^{2-}}$$

$$H_2O + Na^+ + CO_3^{2-} \rightarrow H_2O + Na_2CO_3 \text{ (pH 10.2)}$$

$$H_2O + Na^+ + CO_3^{2-} \rightarrow H_2O + \mathbf{NaHCO_3} \text{ (pH 7.5)}$$

Clearly, a build-up of sodium bicarbonate was occurring in the pond due to the use of CO_2 to lower the pH back to about a pH of 7.

A possible solution would to use HCl to lower pH. The net blow-down to the pond would be NaCl, a desirable byproduct that does not lead to an increase in alkalinity, albeit with a penalty for the cost of HCl.

$$H_2O + Na^+ + OH^- + H^+ + Cl^- \rightarrow \mathbf{H_2O + Na^+ + Cl^-}$$

$$H_2O + Na^+ + OH^- + H^+ + Cl^- \rightarrow \mathbf{H_2O + NaCl}$$

This mechanism was verified on a small scale by flocculating algae at a pH of 10.2 using NaOH. The effluent was isolated and the pH was lowered to 7.0 using HCl (sample 1) and CO_2 (sample 2). As illustrated in the following table, the addition of HCl to lower the pH kept the alkalinity relatively constant while using CO_2 to lower the pH significantly to increase the alkalinity of the effluent.

Table 6. Effect of HCl on alkalinity

	Alkalinity
Water	180 ppm
Sample 1 (HCl)	183 ppm
Sample 2 (CO_2)	448 ppm

Cultivation Duration

The ponds tended to be able to grow consistently for about three months before significant contamination would take over. For example, Pond 4 (greenhouse pond) was inoculated on February 14, 2013, and continued to grow well while continuously harvesting algae. By May 15, Pond 4 had become significantly contaminated with filamentous algae. Growth of Pond 4 was monitored by UV-Vis and by dry weight (DW) and ash free dry weight (AFDW) measurements. As shown in the following plots (**Figure 47**), Pond 4 continued to grow well with continuous harvesting activities.

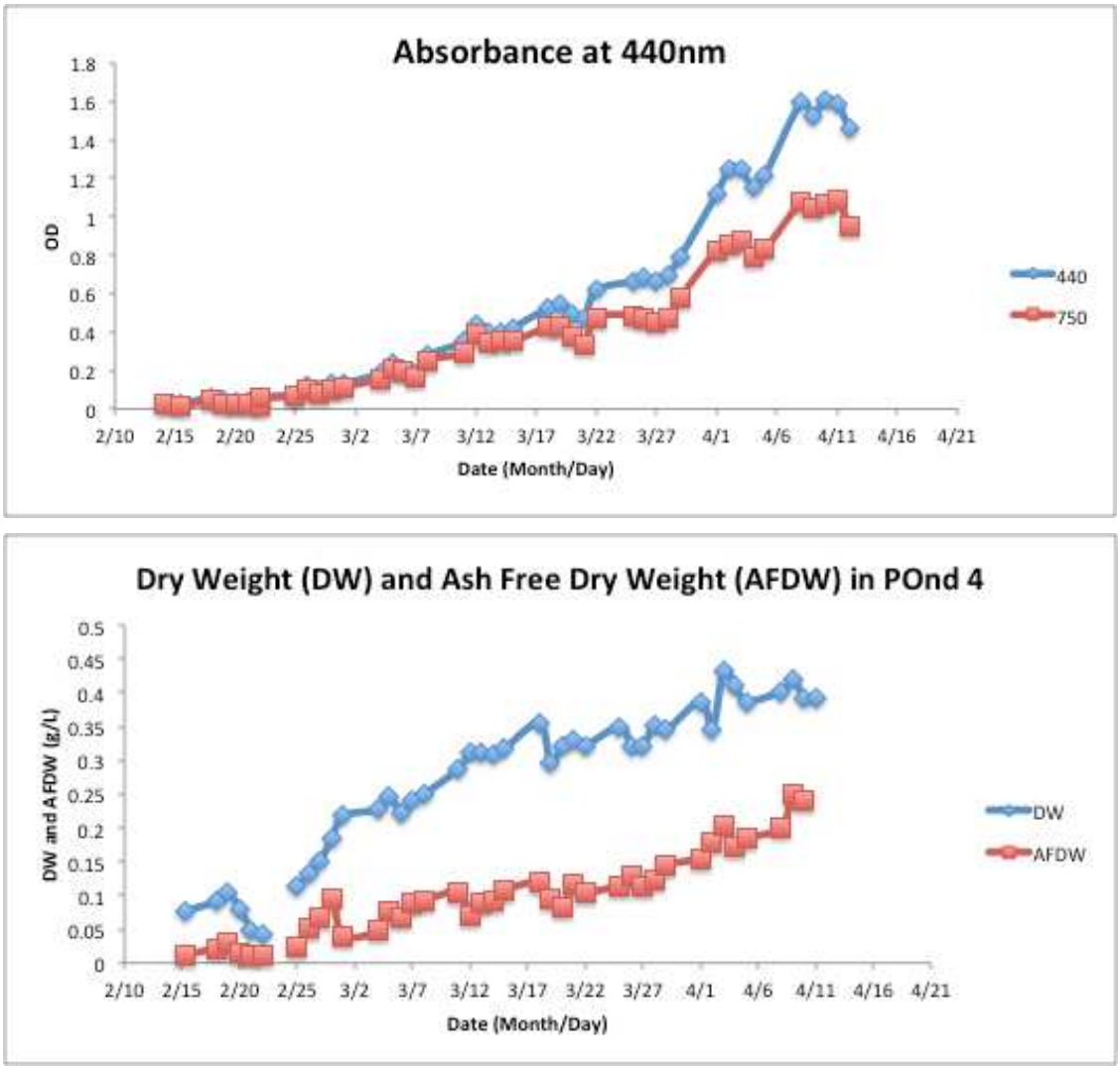

Figure 47. Continuous harvesting activities of Pond 4

By May 15, 2013, Pond 4 began to see increased amounts of contamination with filamentous algae beginning to accumulate on the surface.

About 230,000 liters were harvested from Pond 4 from February 14 – May 15. Harvesting activities produced just over 80 kg DW (dry weight) of algae, and about 57 kg DW algae

remained in the pond. These numbers correlate to about 105 kg of CO_2 utilized for harvested algae and about 180 kg of total CO_2 utilized for total algae growth.

Pond 1 Cultivation

Pond 1 was the outdoor control pond and was inoculated on May 7, 2013 with a starting concentration of about 0.05 g/l. Pond 1 grew very well and was productive until June 19, 2013, at which time the pond crashed. The pond was cleaned and re-inoculated on June 21 with algae from Pond 2. See **Figures 48 and 49** for Pond 1 activity.

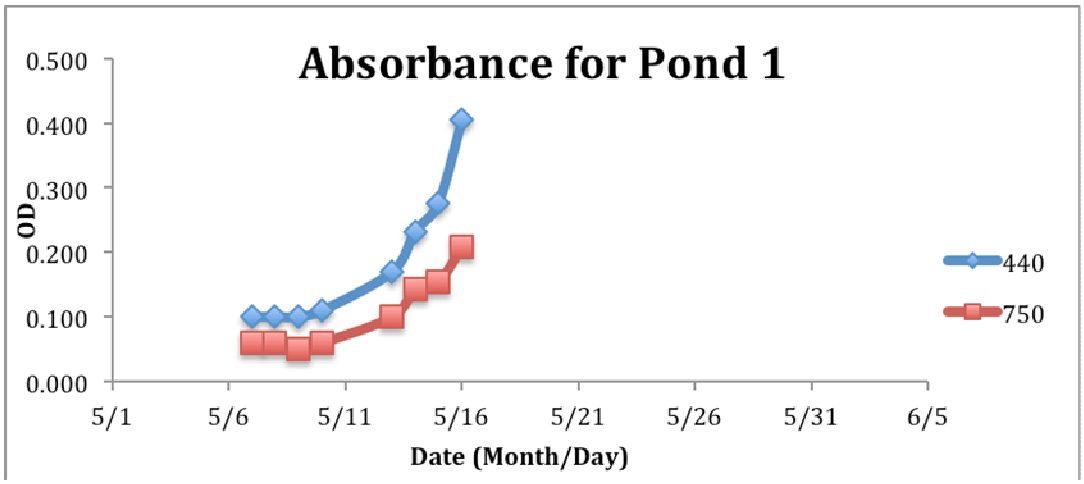

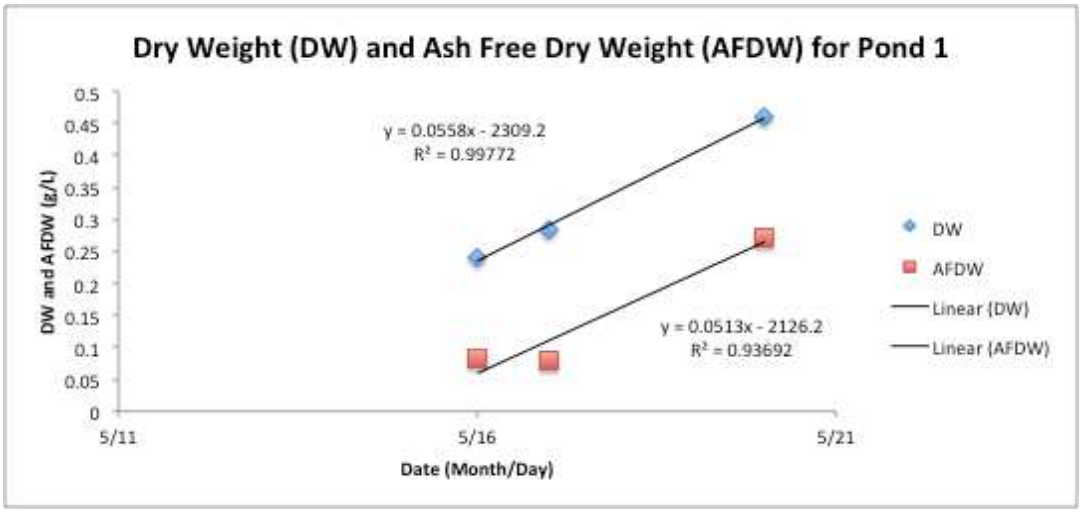

Figure 48. Pond 1 activity

Inoculation of Pond 1 – May 7, 2013

Current - May 16, 2013

Figure 49. Pond 1 inoculation and later results

While Pond 1 was actively growing, 70,686 liters were harvested corresponding to over 32 kg DW of harvested algae. Effluent from the algae concentration unit was treated with HCl rather than CO_2 in an effort to control the alkalinity in the pond. As shown in the alkalinity plot in **Figure 50**, the alkalinity in Pond 1 remained relatively constant. The rise from 350 ppm to about 500 ppm was attributed to a new testing kit with slightly different reagents. All samples recorded higher alkalinity with new test kit.

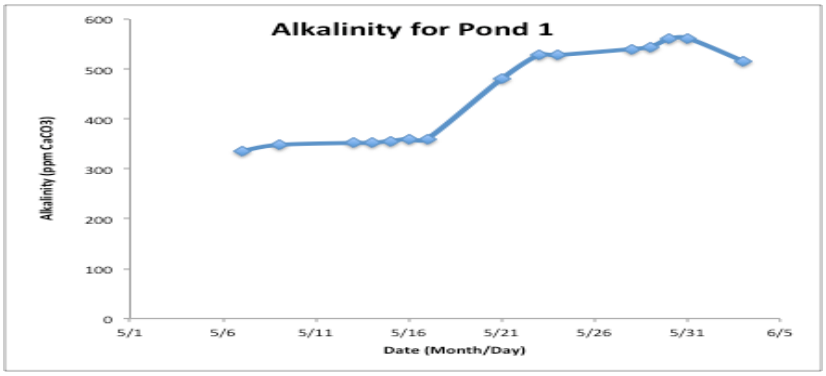

Figure 50. Alkalinity plot for Pond 1

Pond 2 Cultivation

Pond 2 was the PCM pond. The goal was to establish positive algae growth in Pond 2 before layering in the PCM material. Pond 2 was inoculated with algae from Pond 1. The starting concentration was about 0.47 g/l DW. Growth in Pond 2 was monitored by UV-Vis and dry weight and ash free dry weight measurement. The growth rate of Pond 2 (**Figure 51**) was measured at about 0.063-0.076 g/l/day.

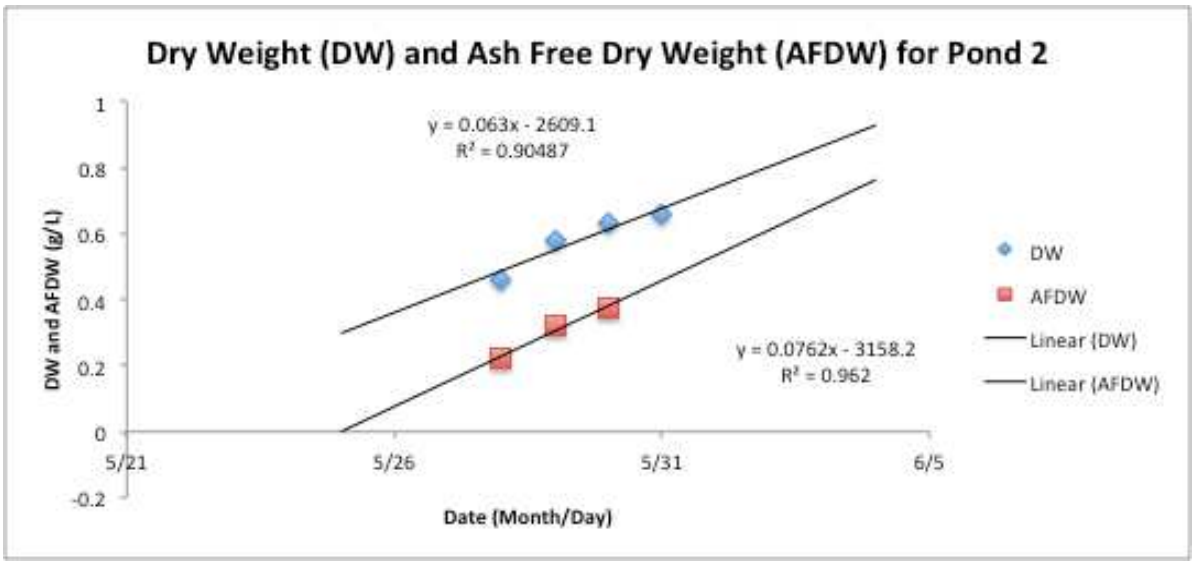

Figure 51. Pond 2 growth rate

PCM Application

Ponds 1 and 2 (outdoor ponds) were inoculated with *nannochloropsis salina* and were allowed to reach a density of about 0.5 g/l. A thin layer of PCM material was applied to the surface of Pond 2. The PCM material had a phase transition point near 60°F (15.5°C), and the thickness of the layer was just under 1/8 of an inch.

Temperature

The temperature of Ponds 1 and 2 was monitored daily along with air and soil temperatures. As shown in **Figure 52**, the temperature of Pond 2 (PCM pond) was consistently higher by about 3°C than that for Pond 1 (control pond). This temperature difference did not appear to increase over time.

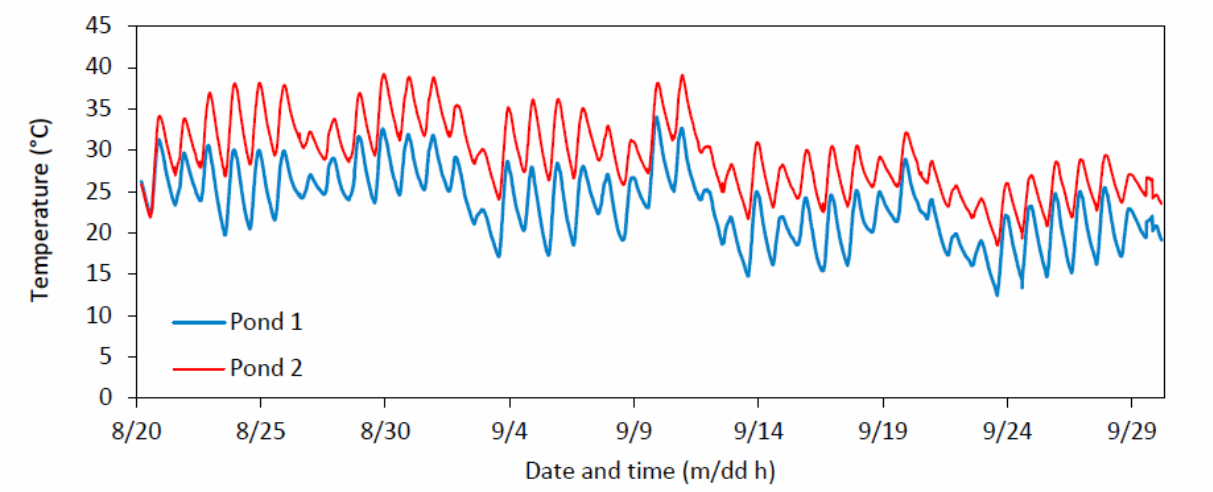

Figure 52. Temperatures of Pond 1 (blue) and Pond 2 (red)

The phase transition point for the PCM material used on Pond 2 was about 18°C. Both air and soil temperatures were consistently above this temperature through September 20. Beyond September 20, the air temperature consistently reached temperatures below 18°C while soil temperatures were generally above 18°C. From September 21 – October 1, the PCM material went through a daily phase transition as the air temperature rose to temperatures above 18°C. As can be seen in **Figure 53**, during the dates in which the PCM material experienced a phase transition (September 21 – October 1), the temperature fluctuations for the PCM pond were not as drastic as those experienced by the control pond. The PCM pond experienced a temperature swing of about 6°C while the control pond showed a temperature swing of about 9°C. It was expected that a thicker layer of PCM material could further reduce the temperature swing of the pond; however, as the PCM layer would thicken, the time required to thaw the PCM layer would increase, as well. Most of the thawing took place during the day when the temperatures rose during the daylight hours. If the layer was too thick and did not thaw relatively quickly upon warming, photosynthetic activity would be reduced.

In the time period before September 21, the PCM pond did not experience consistent phase transitions. As can be seen in **Figure 54**, the temperature fluctuations between Pond 1 (control pond) and Pond 2 (PCM pond) were nearly identical.

For even a small layer of PCM material, less than 1/8 of an inch, the phase transition of the PCM material resulted in reducing the daily temperature swings by about 33%.

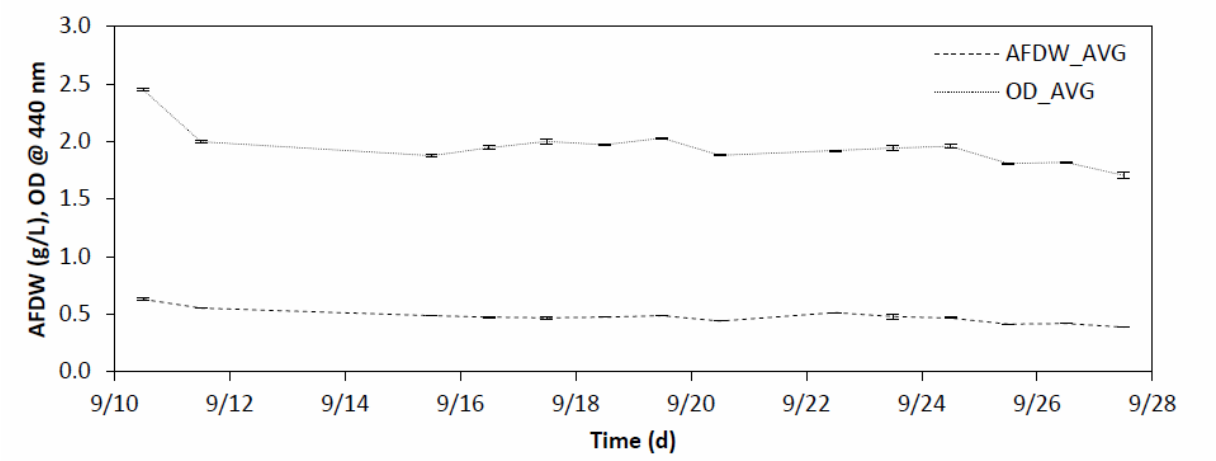

Figure 53. AFDW for Pond 1 (control pond)

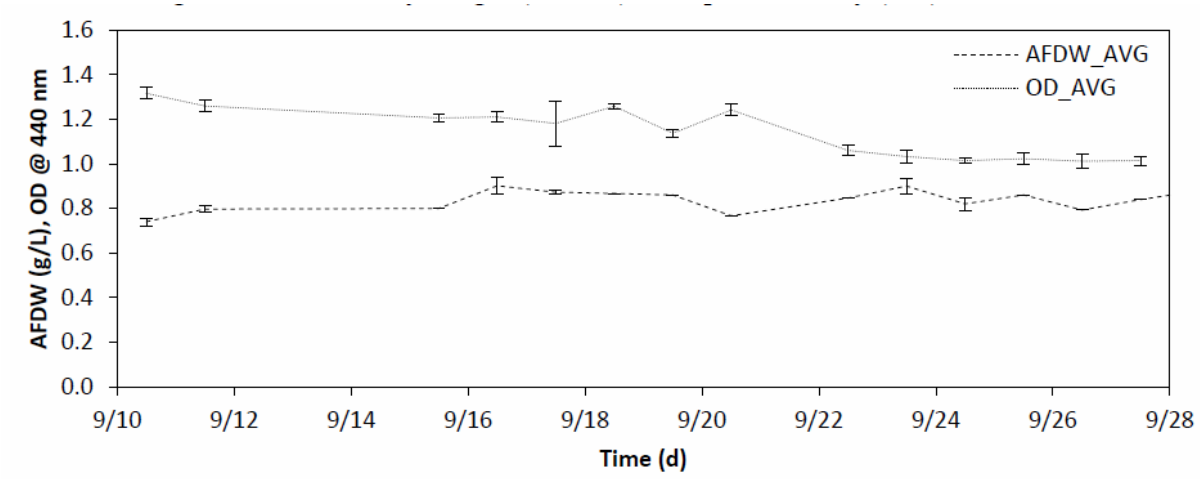

Figure 54. AFDW for Pond 2 (PCM pond)

Algae Growth

Ponds 1 and 2 were both inoculated and monitored until each pond reached a density about 0.5 g/l. With similar starting conditions for each pond, a thin layer of PCM material was added to Pond 2. The layer was just under 1/8 of inch thick. As can be seen in the following figure, Pond 2 (PCM pond) reached a higher level of algae density than that for Pond 1 (control). Pond 2 was able to maintain an algae density of about 0.9 g/l while Pond 1 stayed relatively constant at about 0.5 g/l. Samples were taken in triplicate from multiple locations around each pond.

The density for each pond stayed relatively constant with each pond recovering from harvesting activities within 48 hours. The nominal growth rate for Pond 1 during this time period was about 0.04 g/l/day. The nominal growth rate was based on harvesting 5,000 gallons from Pond 1 every two days at a concentration of 0.5 g/l. The growth rate for Pond 2 (PCM pond) was significantly higher. Harvesting 5,000 gallons every other day at a density of 0.9 g/l resulted in a nominal rate

of 0.08 g/l/day. This conclusion was based on a constant pond volume of 30,000 gallons. Due to minimal water loss for the PCM pond and significant rainfall, the volume of the PCM pond was constantly increasing. During the time period of this study, the PCM pond reached and maintained algae densities 80% greater than the control pond.

Algae Harvesting

Harvesting activities included alternating between Pond 1 and Pond 2. Harvesting volumes were targeted at 5,000 gallons (18,900 liters) corresponding to about 16% of each pond every other day. Pond 1 consistently maintained a density of about 0.5 g/l at the time of each harvest. Pond 1 produced 9.45 kg (AFDW) algae/harvest or 32.4 kg of biomass (29.17% solids). Pond 2 (PCM pond) consistently maintained a density of 0.9 g/l at the time of each harvest. Pond 2 produced 17 kg (AFDW) algae/harvest or 58.3 kg of biomass (29.17% solids). The PCM material provided an 80% increase in harvested algae compared to the control pond.

Semi-continuous Cultivation of *Nannochloropsis salina* in Anaerobic Digestion Effluent

The batch study (previously reported) showed that *N. salina* could adapt to effluent loadings between 3% and 18% (total nitrogen level 80-480 mg/L). The effluent loading of 6% (total nitrogen level 160 mg/L) was chosen for the semi-continuous study because of the relatively high growth rate and biomass yield of *N. salina* under this condition. Different harvesting frequencies (1-, 2-, and 3-day intervals) and harvesting ratios (25% and 50%) were tested for an 18-d culture of *N. salina* (**Table 7**).

Table 7. Experimental design of semi-continuous experiment

Treatment	Harvesting frequency (d)	Harvesting ratio (%)	Hydraulic retention time (d)
1	1	25	4
2	1	50	2
3	2	25	8
4	2	50	4
5	3	25	12
6	3	50	6

As shown in **Figure 55**, at different harvesting frequencies, when half of the culture was harvested each time, the cultures were able to reach steady state earlier than those with 25% of the culture harvested. At a harvesting interval of 1 d, the reactors reached steady state on the second day when half of the culture was harvested, whereas for those with 25% culture harvested, the reactors did not reach steady state until the sixth day. Both harvesting interval and ratio affected the accumulated biomass yield. According to **Figure 56**, at a 25% harvesting ratio, the biomass yield decreased as the harvesting interval increased from 1 d to 3 d, as the hydraulic retention time (HRT) increased from 4 d to 12 d. However, at a 50% harvesting ratio, the highest biomass yield was obtained with a 2-d harvesting frequency at a HRT of 4 days. Although lower harvesting ratios resulted in higher algal cell density, the highest biomass yield during the 18-d continuous cultivation was obtained at a harvesting ratio of 50% and a harvesting interval of 2 d.

(a)

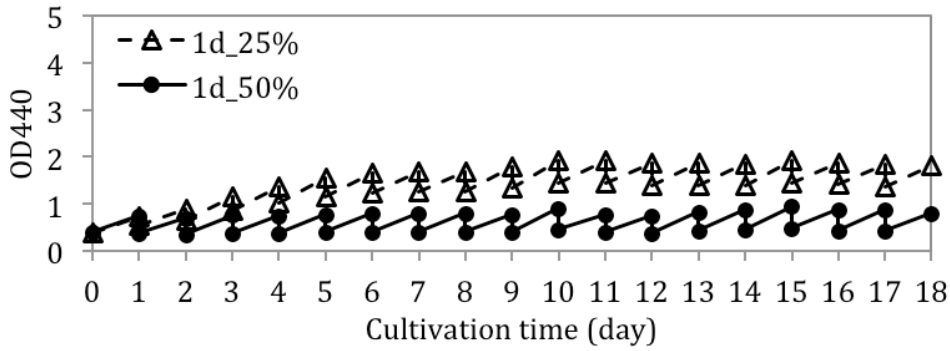

(b)

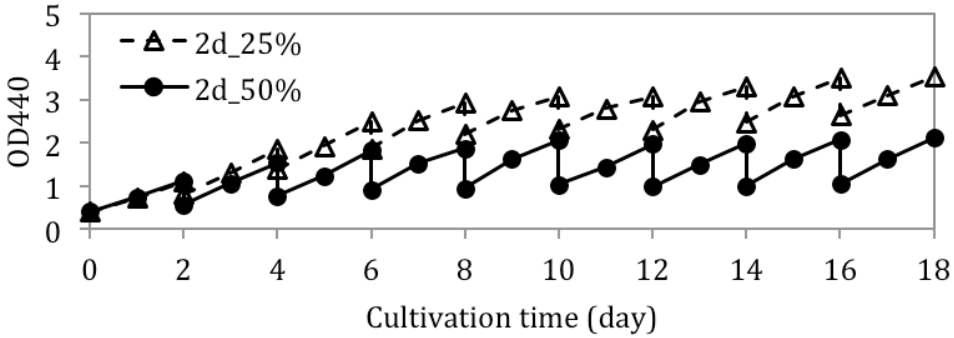

(c)

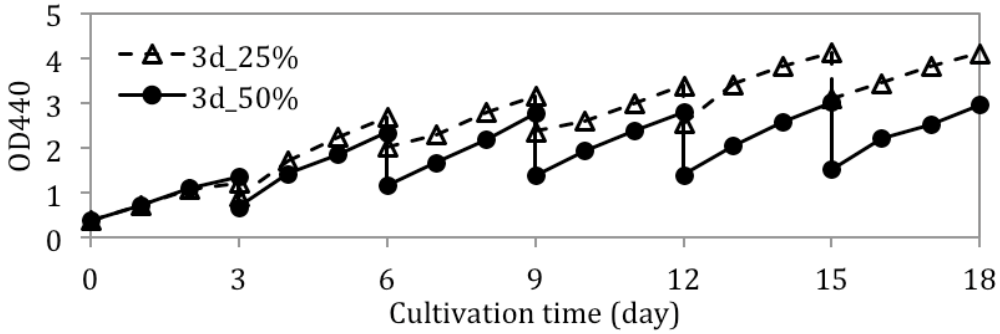

Figure 55. Algal growth curves at different harvesting frequencies and harvesting ratios: (a) harvested every day with 25% or 50% culture removed; (b) harvested every 2 days with 25% or 50% culture removed; (c) harvested every 3 days with 25% or 50% culture removed.

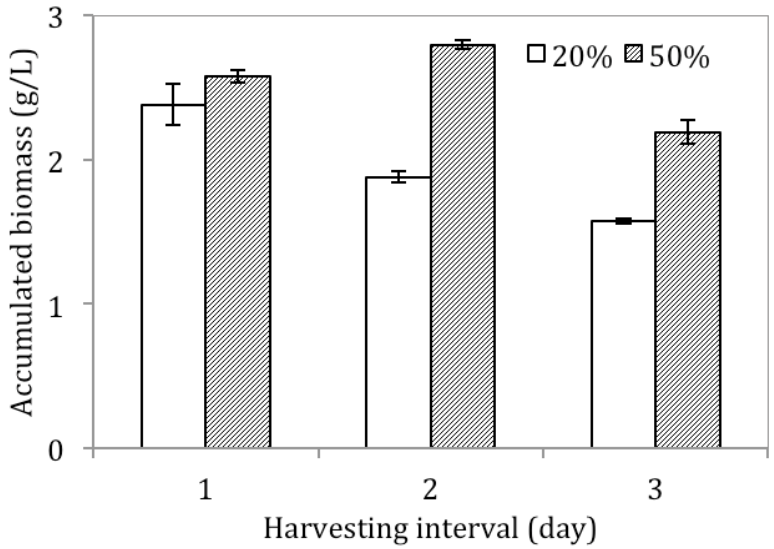

Figure 56. Accumulated algal biomass yield at different harvesting frequencies and harvesting ratios in 18-day semi-continuous cultivation

As shown in **Table 8**, at the same harvesting ratio, the TN removal rate decreased as the HRT increased. Higher harvesting ratios led to higher TN removal rates at each harvesting frequency. The TN removal efficiency was significantly increased as the culture was harvested less frequently ($p < 0.05$) because less frequency resulted in a longer HRT during which more algae biomass would be accumulated and more nutrients could be assimilated. The highest biomass productivity (155.3 mg L^{-1} d^{-1}), lipid content (24.9% AFDW), and lipid productivity (38.7 mg L^{-1} d^{-1}) were obtained at a harvesting ratio of 50% and harvest interval of 2 d (**Table 2**). The maximum lipid productivity of 38.7 mg L^{-1} d^{-1} obtained in the semi-continuous study was 1.33 times of that in the batch study, showing an advantage of semi-continuous cultivation for *N. salina*.

Table 8. Nutrient removal rate and lipid productivity of *N. salina* at different harvesting frequencies and ratios

Harvesting frequency (d)	Harvesting ratio (%)	TN removal rate (mg L^{-1} d^{-1})	TN removal efficiency (%)	TP removal rate (mg L^{-1} d^{-1})	TP removal efficiency (%)	Biomass productivity (mg L^{-1} d^{-1})	Lipid content (% AFDW)	Lipid Productivity (mg L^{-1} d^{-1})
1	25	32.9±3.0	53.5±4.3	4.1±0.3	33.6±2.8	132.1±8.9	18.0±0.6	23.7±2.4
1	50	56.5±4.8	55.2±4.6	4.3±0.4	22.9±2.2	143.0±4.8	19.0±0.4	27.1+1.5
2	25	19.0±2.9	73.4±4.5	3.4±1.1	67.6±3.1	104.3±2.7	19.8±0.9	20.6±1.5

2	50	35.3±4.2	77.8±4.0	3.8±1.2	45.7±6.5	155.3±1.8	24.9±0.5	38.7±2.4
3	25	13.4±2.5	84.7±2.0	2.3±1.6	72.5±5.7	87.4±1.9	18.1±1.1	15.9±1.3
3	50	26.2±2.5	89.0±1.7	3.9±1.3	82.8±1.8	121.4±4.1	22.7±0.4	27.6±1.4

Data are the means ± SE

Anaerobic Digester Effluent as Nutrient Source for Microalgae at Pilot Scale

The purpose of this study was to evaluate the use of wastewater from an anaerobic digester (AD) for the pilot-scale raceway pond cultivation of *N. salina* while simultaneously studying the effect of phase change material (PCM) addition on algae growth, lipid content, and fatty acid methyl ester (FAME) content. The impact of centrate from AD effluent and PCM on algae culture in multiple operating conditions have been evaluated. Preliminary results have displayed a maximum biomass concentration of *N. salina* to be 0.4 grams/liter of total volatile suspended solids (TVSS) when cultured in this wastewater. PCM has displayed control difficulties, with emulsion formation and predator contaminants inhibiting algae growth. Additionally, biomass cultured beneath PCM has much lower eicosapentaenoate (EPA) content, a valuable omega-3 fatty acid. An investigation of centrate from AD effluent versus commercial nutrients in semi-continuous operation is currently being conducted. This investigation was completed on 10/31/2012.

Feed-batch study

Materials and Methods

In order to study the impact of PCM on algae culture with AD effluent as the nutrient source, two raceway ponds were inoculated with *N. Salina*. Effluent from KB Compost Services, Inc.'s Schmack energy anaerobic digester was centrifuged to produce a liquid centrate rich in nutrients. Approximately 160 gallons of centrate from AD effluent were collected from this site in Akron, Ohio on July 2nd, 2012. The feedstock of the anaerobic digestion system was municipal wastewater. Wastewater characteristics of AD effluent centrate were analyzed and are described in **Table 9**.

Table 9. Centrate of AD effluent WW analytes (7/2/2012)

Nutrient Constituent	Concentration (mg/L)
Total nitrogen	6469 ± 90
Total phosphorus	917 ± 23
Ammonia nitrogen	5135 ± 418
Nitrate nitrogen	34.5 ± 3
COD	1550 ± 242

N. Salina was cultured with commercial nutrients in sixteen-2 liter reactors (1 L working volume) in the Bioproducts and Bioenergy Laboratory in controlled conditions. After each reactor reached approximate optical density of 2.0, 14.4 liters of this seed were transferred to one pilot-scale pond at Cedar Lane Farms. The pond was filled with 21 L of centrate of AD effluent in order to reach the predetermined optimum nitrogen concentration of 160 mg/L. Well water was added to reach a final volume of 865 L, and Instant Ocean Sea Salt was introduced to reach a final salinity of 25 parts per thousand (ppt). After *N. salina* concentration in this pond reached approximately 0.1 g/L, it was equally split into two ponds. Both ponds were filled with well water to 865 L, required salt to reach equivalent salinity of 25 ppt, and approximately 19 L of AD effluent centrate to reach equivalent concentrations of 160 mg/L total nitrogen. One pond was covered with a ½ inch layer of phase change material (PCM). The second pond served as the control without PCM. Temperature, pH, salinity, and dissolved oxygen were measured daily to monitor the process. Optical density (@ 440 nm wavelength) and total volatile suspended solids (TVSS) were measured to evaluate the algae growth. Total nitrogen (TN) was determined with a HACH Spectrophotometer to monitor nutrient levels. According to measured TN concentrations, centrate of AD effluent was added to replenish nutrients back to 160 mg/L. This process continued for 10 days until the control pond reached a constant maximum optical density and total volatile suspended solids concentration.

Results and Discussion

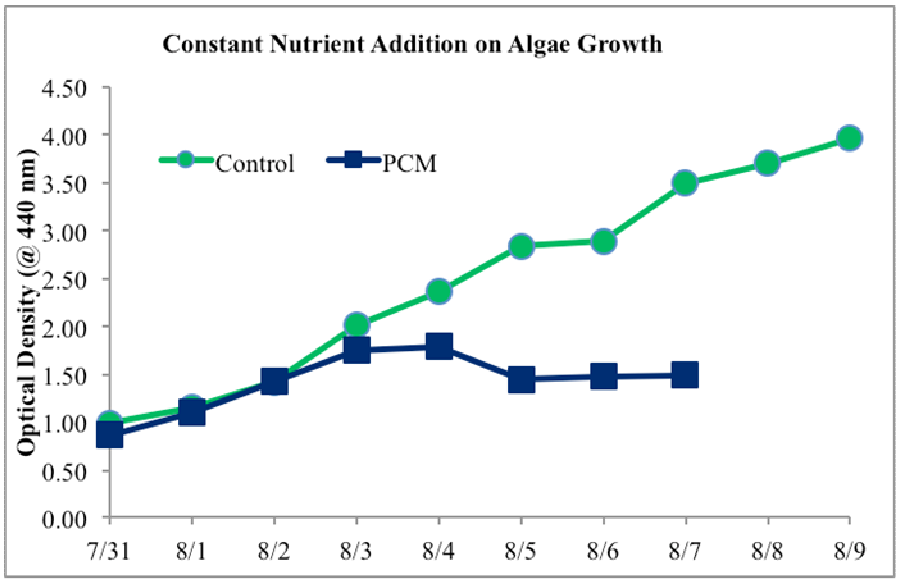

Figure 57. Algae growth curve with and without PCM in constant nutrients experiment

As displayed in **Figure 57** above, both ponds followed similar growth conditions until 8/3/2012. At the 865 L water level (8-inch pond depth), control of the PCM with baffle was inadequate, and an emulsion layer of PCM was formed that inhibited *N. salina* growth. Additionally, predator contaminants were identified in the PCM pond. The control pond exhibited typical biological growth kinetics, with a lag, exponential growth, and stationary phases throughout the 17-day fed batch operation, with a maximum biomass concentration measured at 0.4 g/L

(OD=4). The doubling time of the control pond biomass concentration was determined to be 3.41 days.

Semi-continuous experiment

Experimental Design

In the second run of experiments (see **Figure 58**), the start-up procedure was similar to the first run of experiments in which two raceway ponds were inoculated with *N. Salina* to an optical density (OD) of approximately 1.50. Both of the ponds were filled to 1395 liters to utilize the baffles and solve the PCM emulsion issue encountered in the first experiment. Ponds were dosed with 1% by volume (13.95 L) of centrate of AD effluent after each harvest (every 2 days). The harvest ratio was determined to be ½ of the pond volume. A ½ inch layer of PCM was added to the experimental pond. The second pond served as the control without PCM. Measurement procedures used were the same as the first run.

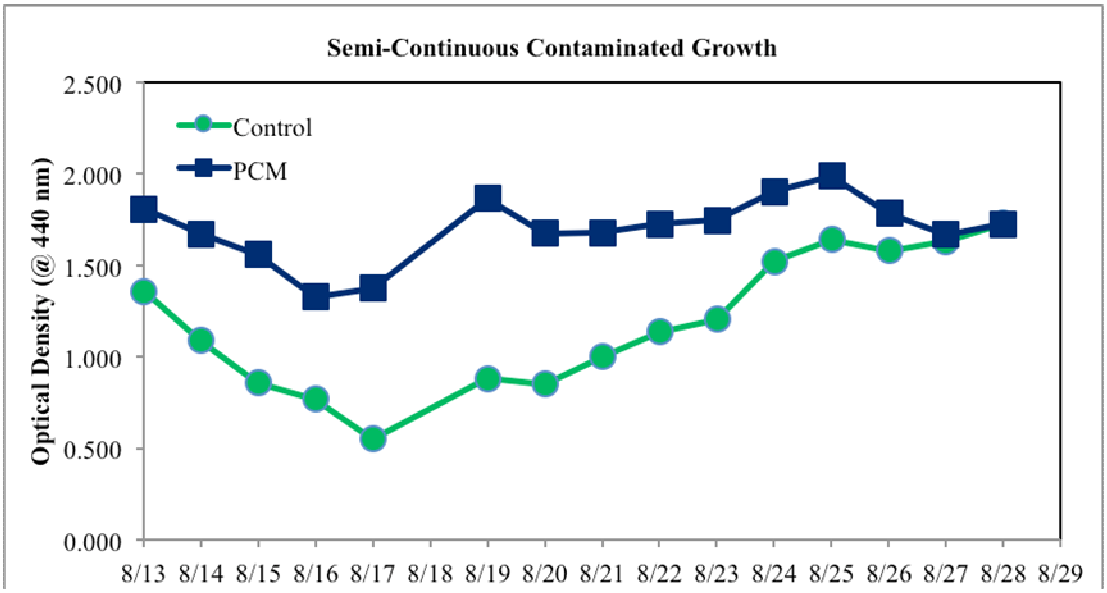

Figure 58. Algae growth curve with and without PCM in semi-continuous experiment

Results and Discussion

The first dosing of centrate from AD effluent for both ponds began on 8/13/2012. After two days, ½ of the pond volumes were harvested via centrifuge. The biomass collected from each pond was analyzed for lipid and fatty acid methyl ester (FAME) content. These results are shown in **Figure 59**.

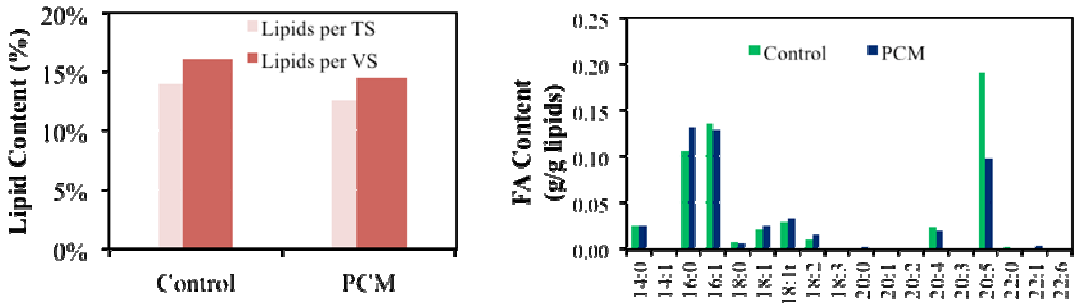

Figure 59. Algae lipid and FAME contents in semi-continuous experiment

Figure 59 displays that lipid content was not greatly affected by the addition of PCM. In terms of total volatile solids, the lipid content in the control pond was 16.07% compared to the PCM pond with 12.60%. The PCM pond showed a drastic decrease in the FAME eicosapentaenoate (EPA), with other FAME's remaining similar to the control pond results.

After harvesting on 8/15/2012, an influx of predator contaminants in the form of ciliates, flagellates, amoeba, and other algae caused a rapid inhibition of *N. salina* growth. Due to this inhibition, harvesting ceased, and bi-daily feeding of AD centrate was continued in order to monitor contaminant species. As displayed in **Figure 58**, *N. salina* was unable to return to exponential growth after the influx of contaminant species.

Restart of the Semi-continuous Test

In order to study the feasibility of growing microalgae using effluent as nutrient source, two raceway ponds were inoculated with *N. Salina* in similar conditions to previous experiments. A new batch of AD effluent centrate was collected on 9/11/2012 from KB Compost Services, Inc.'s Schmack Energy anaerobic digestion system in Akron, Ohio. The feedstock of the anaerobic digestion system was municipal wastewater. Total nitrogen, total phosphorus, ammonia nitrogen, nitrate nitrogen, and TKN concentrations were evaluated and are described in **Table 10**.

Table 10. Centrate of AD effluent WW constituents (9/11/2012)

Nutrient Constituent	Concentration (ppm)
Total Nitrogen	2897 ± 87
Total Phosphorus	425 ± 1
Ammonia Nitrogen	2845 ± 25
Nitrate Nitrogen	9.30 ± 1
TKN	2850 ± 50

This batch of effluent was fed to microalgae on 9/13/2012. However, due to unknown inhibitory components, microalgae growth was inhibited. After 2 weeks of dormancy, the microalgae recovered. Therefore, a new semi-continuous experiment was designed. One pond was dosed

with commercial nutrients while an experimental pond was dosed with this new AD centrate at low dose (0.4% by volume). Harvest ratios were set to ¼ of the pond volume (1030 L) every 3 days. Preliminary observations have shown AD centrate-induced ponds to be attractive to predator contaminants while commercial nutrients have allowed *N. salina* to remain the dominant species in culture.

Anaerobic Digester Effluent as Nutrient Source for Microalgae at Pilot Scale

The purpose of this study was to evaluate the use of wastewater from an anaerobic digester (AD) for the pilot-scale raceway pond cultivation of *Nannochloropsis salina.* The study attempted to compare AD effluent with traditional commercial nutrients on algae growth, lipid content, and fatty acid methyl ester (FAME) content. The impact of AD effluent on algae culture in multiple operating conditions in the autumn and winter months has been evaluated. October conditions displayed a maximum biomass productivity of *N. salina* to be 0.18 g L^{-1} d^{-1} of total volatile suspended solids (TVSS) and lipid content of 26% by dry weight for commercial nutrient media. November growth was very limited with a 0.07 g L^{-1} d^{-1} biomass productivity and lipid content of 17% by dry weight for commercial nutrient media. Growth in AD effluent was significantly lower under the same conditions. A lab-scale investigation of the effects of nutrient concentration, light cycles and temperature variance on *N. salina* was then conducted in order to provide insight to the limiting factors in outdoor cultivation systems.

Autumn Semi-Continuous Study

Materials and Methods

In order to study the impact of nutrient sources, two raceway ponds were inoculated with *N. Salina*, one pond fed with AD effluent and the second pond fed with commercial nutrients. Effluent from KB Compost Services, Inc.'s Schmack energy anaerobic digester was centrifuged to produce a liquid centrate rich in nutrients. Approximately 140 gallons of centrate from AD effluent were collected from this site in Akron, Ohio on September 11th, 2012. The feedstock of the anaerobic digestion system was municipal wastewater. Wastewater characteristics of AD effluent centrate were analyzed and are described in **Table 11**.

Table 11. Centrate of AD effluent WW analytes (9/11/2012)

Nutrient Constituent	Concentration (ppm)
Total Nitrogen	2897 ± 87
Total Phosphorus	425 ± 1
Ammonia Nitrogen	2845 ± 25
Nitrate Nitrogen	9.30 ± 1
TKN	2850 ± 50

This batch of effluent was fed to microalgae on 9/13/2012. However, due to unknown inhibitory components, microalgae growth was inhibited. After 2 weeks of dormancy, the microalgae

recovered. Therefore, a new semi-continuous experiment was designed. *N. Salina* was cultured in both ponds until the biomass density of each was 0.2 g/L of TVSS. One pond was fed with commercial nutrients while an experimental pond was fed AD effluent at low dose (0.4% by volume). Harvest ratios were set to ¼ of the pond volume (1030 L) every 3 days until the retention time was complete (12 days). Each harvest was analyzed for lipid and fatty acid methyl ester (FAME) concentration. Cultures were continued for two further harvests to verify results. This experimental trial was repeated during the month of November.

October Trial Results and Discussion

As displayed in **Figure 60**, biomass accumulation was significantly higher in the commercial nutrient pond (P2) than in the AD effluent pond. Pond 2's biomass accumulation was low at 3.2 g L^{-1} of TVSS, corresponding to a volumetric productivity of 0.18 g L^{-1} d^{-1}. Pond 1 accumulation was 2.1 g L^{-1} corresponding to a volumetric productivity of 0.12 g L^{-1} d^{-1}. There was a decline in measured biomass density over the time period, which can be attributed to several factors. High concentrations of ciliates were observed in the AD effluent pond from the beginning of this trial, with contaminants entering the commercial nutrients pond on 10/21. The culture stabilized around 10/26, indicating the ecosystem had adapted to the harvesting conditions set for this experiment. Additionally, there was fluctuation in pond temperatures over the course of this trial from 15-20°C, which likely had an impact on algae growth in both culture conditions.

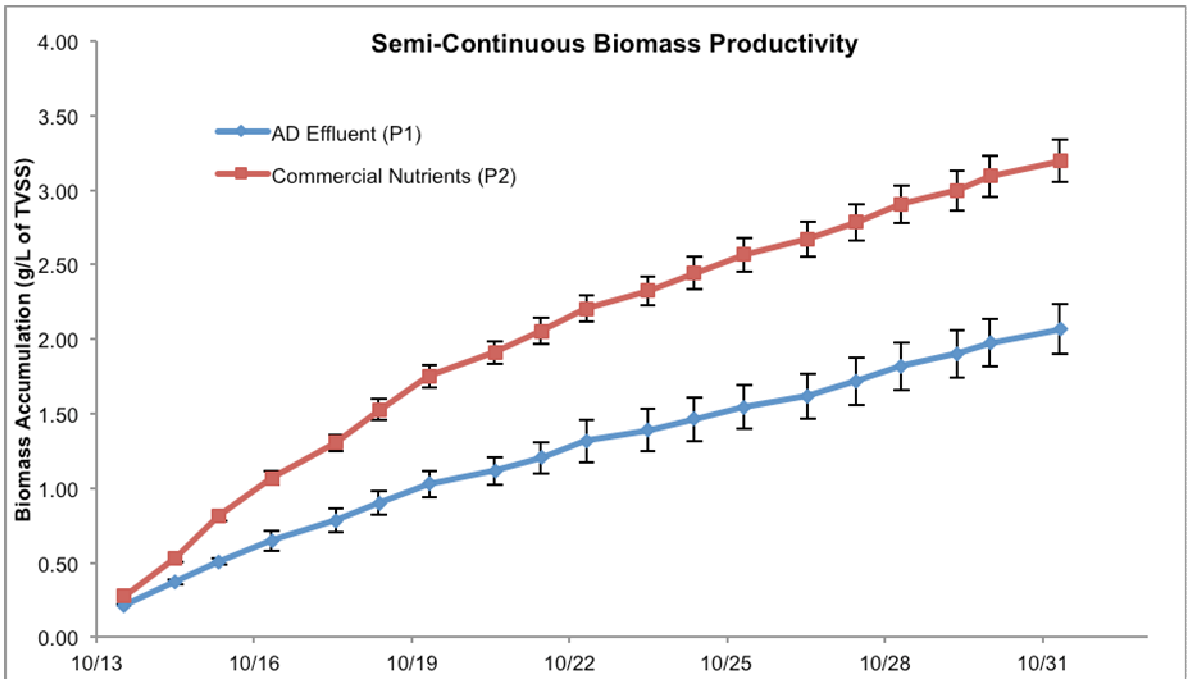

Figure 60. Biomass productivity in semi-continuous conditions (October)

Figure 61 displays the lipid and FAME analysis from the semi-continuous trial in October, 2012. The average lipid content for both ponds was roughly 26% of lipids by dry weight. The average FAME concentration was 47% of FAME per dry lipids for the AD effluent pond and 57% for the

commercial nutrient pond. Statistical analysis (*t*-test α=0.05) showed the commercial nutrient pond had statistically higher lipid and FAME contents than the AD effluent pond at harvest 1. Analysis of lipid and FAME results showed no significant difference between commercial nutrients and AD effluent for harvests 3 and 4. This result can be attributed to the drastically higher concentrations of ciliate predators in the AD effluent pond at this harvest date. Additionally, the eicosapentaenoic acid (EPA) concentration also declined with predator concentration, as EPA concentration was statistically higher in the commercial nutrient pond for harvests 1 and 2. The structure of the biomass was also impacted by predator contaminants (see **Figure 62**). As seen in the photo of biomass from harvest 1, the normally thick dark biomass of *N. salina* became light green and obtained much more moisture.

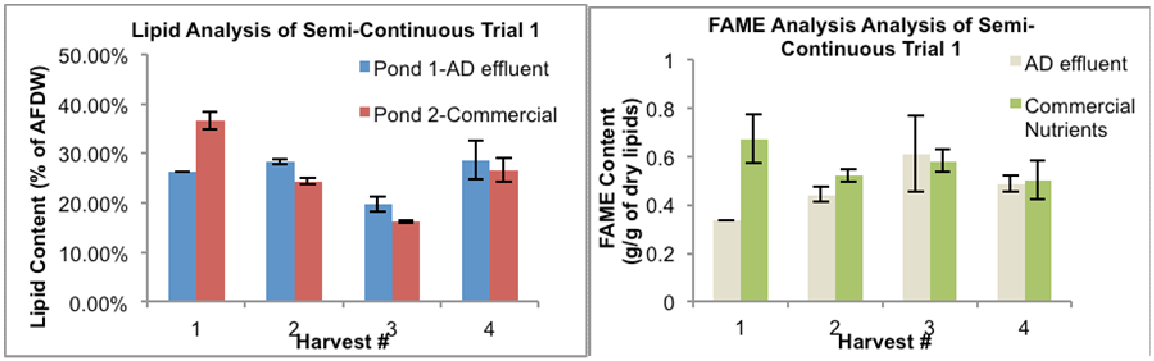

Figure 61. Algae lipid and FAME contents in semi-continuous experiment

Figure 62. Contaminant effect on biomass structure

Dry lipid productivity was 0.030 g L^{-1} d^{-1} for the AD effluent pond and 0.046 g L^{-1} d^{-1} for the commercial nutrients pond. FAME productivity was 0.014 g L^{-1} d^{-1} for the AD effluent pond and 0.026 g L^{-1} d^{-1} for the commercial nutrients pond.

Semi-Continuous Trial

After completion of the October trial, this experiment was repeated during the month of November. The trends were similar, as biomass accumulation declined to approximately1.1 g L^{-1} for the commercial nutrient pond and 0.7 g L^{-1} for the AD effluent pond, with productivities of 0.07 g L^{-1} d^{-1} and 0.05 g L^{-1} d^{-1}, respectively. Lipid concentrations declined over the growth period. The average lipid content was 16% for the November trial, with FAME analysis not

conducted. Predators continued to be prevalent, although their impact was not as severe during the November experiment. Seasonal variation during November 2012 was much more severe with temperature ranging from 13 to 18°C. Additionally, nitrogen concentration was not depleted during the course of this trial, indicating nutrient levels were not the primary impact of biomass decline. Rather, it was hypothesized that light availability and temperature have the greatest effect on *N.salina* biomass growth. Therefore, a new set of experiments was designed to quantify the impacts of nutrient concentration, temperature, and light availability on the growth of this strain.

Two lab-scale experiments were conducted to quantify the effects of nutrient loading, temperature, and light availability on the growth of *N. salina*.

Loading Rate Experiment
In order to quantify the effects of nutrient loading, 10 dilutions of AD effluent were fed to algae under continuous illumination in a 10-day batch regime. Preliminary results from this experiment showed that total nitrogen concentration of 200 mg/L had the highest growth rate. This information was utilized for the light-cycle experiment discussed below. This experiment was conducted with commercial nutrients to make an adequate comparison between both nutrient sources.

Light-Cycle Temperature Variance Experiment
In order to quantify the effects of seasonal variance on the growth of *Nannochloropsis salina*, controlled variance of four temperature conditions (15, 20, 25, 30°C) and three light availabilities (6:18, 12:12, 24:0) wee tested at the optimum nutrient loading of AD effluent (200 mg/L of TN). Light cycles are in terms of hour light: hour dark. Preliminary results from this experiment show that light availability has the primary impact on the growth of this strain. Additionally, the results have shown good correlation with pilot pond data collected during the summer of 2012.

Effect of AD Effluent as a Nutrient Source and Light Availability on Lipid and Fatty Acid Methyl Ester (FAME) Content
Previously, AD effluent had been compared with commercial f/2 media on algae biomass growth and nitrogen removal under a variety of light and temperature conditions. In this study, the effect of nutrient source and light availability on lipid and FAME content of *N. salina* was further evaluated.

Materials and Methods
Lipid content of the microalgae biomass was analyzed using a modified version of Folch's method (Folch et al., 1957). 7 mL of methanol was added to 1.0-2.0 g of thickened biomass sample. Before extraction, the cells were disrupted with a UP400S ultrasonic processor (Hielscher Ultrasonics, Teltow, Germany) and an H22 titanium sonotrode with a 22 mm tip. The frequency of the ultrasound was set at 24 kHz and the output was set at 100 W. 14 mL of chloroform was added to the sample and disrupted again with the ultrasonic processor. Lipids were extracted by mixing chloroform-methanol (2:1 v/v) with the samples. Water with a KCl content of 0.88% by weight was added to give a final solvent ratio of chloroform: methanol: water of 8:4:3. The sample was placed in a capped centrifuge tube and shaken manually for 10 min. The mixture was then centrifuged for 5 min at 1000 x g. The top layer of the mixture (water

and methanol) was removed with a pipette. The biomass layer and the chloroform layer were filtered using Whatman No. 1 filter paper (GE Healthcare, Maidstone, UK). The tube and filter paper were washed with 20ml of chloroform to collect residual lipids. The chloroform was evaporated using a rotary evaporator. The weight of the crude lipid obtained from each sample was measured using an electronic scale.

FAME analysis was conducted on each lipid sample according to Li and Watkins (2001) by saponifying lipid samples with 0.5 N sodium hydroxide (NaOH) in methanol at 100°C for 5 min. The liberated fatty acids were then methylated in 14% boron trifluoride (BF3) in methanol at 100°C for 5 min. The resulting fatty acid methyl esters (FAMEs) were extracted with hexane and quantified by a gas chromatograph-mass spectrometer (GC-MS), GCMS-QP2010 SE unit (Shimadzu, Columbia, MD, USA), equipped with a ZebronTM ZB-FFAP polar capillary column (Phenomenex, Torrence, CA, USA). Helium was used as the mobile phase at a flow rate of 1 ml min^{-1}. The oven temperature was raised from 50°C to 190°C at a rate of 25°C min-1, then to 220°C at a rate of 3°C min-1, and then held for 18 min. The injector, interface, and ion source temperatures were held at 250°C, 250°C, and 200°C, respectively. FAME samples of 1µL each were injected with a split ratio of 50:1. The compounds were identified in the National Institute of Standards and Technology (NIST) Mass Spectral Database and quantified by comparing the peak area with 100µg/mL of methyl heptadecanoate as an internal standard. The cetane number of total fatty acids was calculated according to Piloto-Rodriguez et al. (2013).

Results and Discussion

Lipid and FAME analysis between culture systems and nutrient source for *N. salina* is highlighted in **Table 11**.

Table 11. Lipid and FAME Analysis

	Constant Illumination (mimic photobioreactors)		**Variable Illumination (mimic open raceway ponds)**	
	Commercial nutrients	**AD effluent**	**Commercial nutrients**	**AD effluent**
Lipid Content ($g\ g^{-1}$ TVS)	0.263 ± 0.033	0.261 ± 0.003	0.262 ± 0.049	0.317 ± 0.020
Total Fatty Acids (TFAs) ($g\ g^{-1}$ lipids)	0.661 ± 0.006	0.575 ± 0.043	0.632 ± 0.024	0.617 ± 0.042
Total Saturated FAs ($g\ g^{-1}$ TFAs)	0.320 ± 0.004	0.344 ± 0.001	0.286 ± 0.006	0.274 ± 0.006
Total Unsaturated	0.680 ± 0.004	0.656 ±	0.714 ± 0.006	0.726 ± 0.006

FA's (g g^{-1} TFAs)		0.001		
FAME Constituent (% of TFAs)				
C 14:0	7.98 ± 0.13	7.79 ± 0.07	7.08 ± 0.14	7.26 ± 0.16
C 14:1	0.43 ± 0.04			
C 16:0	21.60 ± 0.04	23.74 ± 0.28	18.90 ± 0.27	18.19 ± 0.22
C 16:1	25.18 ± 0.83	24.88 ± 0.85	24.66 ± 0.27	26.40 ± 0.30
C 18:0	2.46 ± 0.31	2.87 ± 0.32	2.63 ± 0.26	1.96 ± 0.20
C 18:1	4.99 ± 0.57	5.96 ± 0.44	4.98 ± 0.11	3.91 ± 0.18
C 18:1t		3.19 ± 0.22	1.80 ± 0.12	1.27 ± 0.05
C 18:2	2.09 ± 0.04	2.44 ± 0.11	2.50 ± 0.06	2.98 ± 0.05
C 20:0				
C 20:2				
C 20:4	4.51 ± 0.13	3.47 ± 0.01	4.67 ± 0.09	4.97 ± 0.02
C 20:3				
C 20:5 EPA	30.78 ± 0.08	25.66 ± 0.21	32.79 ± 0.65	33.07 ± 0.02
Cetane Number	55.28 ± 0.24	56.02 ± 0.01	54.50 ± 0.21	54.09 ± 0.19

Statistical analysis revealed several interesting trends between culture system and nutrient source. Lipid content and total fatty acids were unaffected by culture system and nutrient source, indicating that open raceway ponds fed diluted AD effluent can obtain similar lipid productivities to open raceway ponds using commercial nutrients. Under the same light condition, the saturated or unsaturated fatty acid contents for the algae fed with diluted AD effluent were comparable to those fed commercial nutrients. However, light conditions affect saturated fatty acid content. Algae culture under varied illumination had 11-20% less saturated fatty acid (mainly due to the difference in C16:0) than constant intensity cultures. Varied illumination also increased unsaturated fatty acid content. For example, the C20:5 (EPA) and C20:4 content of algae culture under varied illumination were 29 and 43% higher than those

under constant illumination, respectively. Higher content of palmitate (C 16:0) in algae cultures under constant illumination caused a slightly higher cetane number for both nutrient sources.

The ratio of C 16:1 to C 16:0 in the cultures declined from approximately 1.4 to 1.0 under constant illumination of 200 µmol m^{-2} s^{-1} using either commercial nutrients or AD effluent as a nutrient source. This number indicates that the amount of nutritional FAMEs may decline at high light intensity. Increased values of C 16:0 caused an increase in the cetane number of biodiesel. Therefore, varied light intensity in open systems may improve the concentration of valuable unsaturated fatty acids. In Touchstone's experiments, biomass productivity was similar in varied and constant illumination culture systems, with higher monounsaturated fatty acids in varied illumination conditions.

The results from **Table 11** indicate several advantages of *N. salina* cultivated in open raceway ponds. Current literature concluded that microalgae for biodiesel are currently not cost-effective, and culture systems focusing on production of high-quality, unsaturated fatty acids for nutritional supplements and aquaculture feed could bridge the economic gap. Additionally, Touchstone's experimental results show no statistical difference between *N. salina* fatty acid production when cultivated in diluted anaerobic digester effluent and commercial f/2 media at equivalent nitrogen concentrations. Open raceway ponds using diluted AD effluent could improve the economics of the production of microalgae biomass.

Kinetic Algae Growth Model and Validation with Large-scale Pond Setup

The purpose of this study was to develop and evaluate the simulated algae growth in an open pond using a series of kinetic equations, which depict the change in biomass and nutrient concentrations, and a computational fluid dynamics (CFD) model, which takes account for the irregular fluid flow and mass transport within the system. By effectively predicting the behavior of algae growth dependent on environmental conditions such as temperature, nutrient concentrations, irradiance, and flow conditions, large-scale productivity can be estimated without the consumption of valuable resources and energy.

Model setup

Kinetic model

The photosynthetic microalgae growth system of microalgae can be assumed to be a chemostat with a steady inflow and outflow of pond medium. The flux of biomass, CO_2 concentration, and nitrogen concentration can be expressed in the form of ordinary differential equations, and, thus, the kinetic balance of the system can be determined by solving the array of equations, shown below.

$$\begin{cases} \dfrac{dX}{dt} = \dfrac{F}{V}(X_0 - X) + \hat{\mu}\left(\dfrac{C}{K_C + C}\right)\left(\dfrac{N}{K_N + N}\right)\left(\dfrac{\bar{I}}{K_I + \bar{I}}\right)e^{-i(\bar{I} - I_{opt})^2}X - DX & (1) \\ \dfrac{dC}{dt} = \dfrac{F}{V}(C_0 - C) + \dfrac{6nQ_0D_C}{ud_b^2}\left[2 + 0.015\left(\dfrac{\rho u d_b}{\mu_L}\right)^{0.89}\left(\dfrac{\mu_L}{\rho D_C}\right)^{0.7}\right](C^* - C) - \mu X Y_{C/X} & (2) \\ \dfrac{dN}{dt} = \dfrac{F}{V}(N_0 - N) - \mu X Y_{N/X} & (3) \end{cases}$$

where $X \equiv$ effluent mass concentration of algae (g m^{-3})
$F \equiv$ mass flow rate of effluent (m^3 d^{-1})
$V \equiv$ volume of pond segment (m^3)
$X_0 \equiv$ influent mass concentration of algae (g m^{-3})
$\hat{\mu} \equiv$ maximum specific growth rate (d^{-1})
$C \equiv$ concentration of dissolved CO_2 (g m^{-3})
$K_C \equiv$ half-saturation constant for cell growth dependent on CO_2 (g m^{-3})
$N \equiv$ concentration of inorganic nitrogen (g m^{-3})
$K_N \equiv$ half-saturation constant for cell growth dependent on N (g m^{-3})
$\bar{I} \equiv$ average irradiance between the surface and bottom of pond (MJ m^{-2} d^{-1})
$K_i \equiv$ half-saturation constant for cell growth dependent on average irradiance (MJ m^{-2} d^{-1})
$j \equiv$ empirical constant for non-optimal temperature
$T \equiv$ temperature (°C)
$T_{opt} \equiv$ optimal temperature for autotrophic growth
$D \equiv$ death coefficient (d^{-1})
$C \equiv$ concentration of dissolved CO_2 (g m^{-3})
$C_0 \equiv$ influent concentration of CO_2 (g m^{-3})
$n \equiv$ number of orifices per unit area (m^{-2})
$Q_0 \equiv$ Total volumetric flow rate of inflowing CO_2 (m^3 s^{-1})
$D_C \equiv$ diffusivity of CO_2 in water (m^2 d^{-1})
$u \equiv$ ascension velocity of bubble in water (m s^{-1})
$d_b \equiv$ bubble diameter (m)
$\rho \equiv$ density of liquid phase (kg m^{-3})
$\mu_L \equiv$ dynamic viscosity of liquid phase (kg m^{-1} s^{-1})
$C^* \equiv$ saturation concentration of dissolved CO_2 (mg l^{-1})
$\mu \equiv$ specific growth rate of algae (d^{-1})
$Y_{C/X} \equiv$ mass of CO_2 consumed per unit mass of microalgae
$N \equiv$ concentration of inorganic nitrogen (g m^{-3})
$N_0 \equiv$ influent concentration of nitrogen (g m^{-3})
$Y_{N/X} \equiv$ mass of nitrogen consumed per unit mass of microalgae

Incorporating into CFD model
The 3-D environment and mesh was created with the CFD software ANSYS® Fluent (**Figure 63**). Using a tetrahedral mesher, a total of 23422 nodes and 89447 elements were created. A standard *k-ε* model was used with a Reynolds number of approximately 20000. The turbulence kinetic energy, *k*, and its rate of dissipation, *ε*, were obtained from the following transport equations:

$$\frac{\partial}{\partial t}(\rho k) + \frac{\partial}{\partial x_i}(\rho k u_i) = \frac{\partial}{\partial x_j}\left[\left(\mu + \frac{\mu_t}{\sigma_k}\right)\frac{\partial k}{\partial x_j}\right] + G_k + G_b - \rho\varepsilon - Y_M + S_k$$

$$\frac{\partial}{\partial t}(\rho \varepsilon) + \frac{\partial}{\partial x_i}(\rho \varepsilon u_i) = \frac{\partial}{\partial x_j}\left[\left(\mu + \frac{\mu_t}{\sigma_\varepsilon}\right)\frac{\partial \varepsilon}{\partial x_j}\right] + C_{1\varepsilon}\frac{\varepsilon}{k}(G_k + C_{3\varepsilon}G_b) - C_{2\varepsilon}\rho\frac{\varepsilon^2}{k} + S_\varepsilon$$

where G_k represents the generation of turbulence kinetic energy due to the mean velocity gradients, G_b represents the generation of turbulence kinetic energy due to buoyancy, Y_M represents the contribution of the fluctuating dilatation in compressible turbulence to the overall

dissipation rate, C_1, C_2, and C_3 are constants, and σ_k and σ_ε are the turbulent Prandtl numbers for k and ε, respectively. The boundary conditions for the model include a tangential fluid velocity of 0.3 m/s along the paddle wheel contact surface, a free fluid surface with a constant temperature of 20°C and no-slip wall conditions for the pond interior.

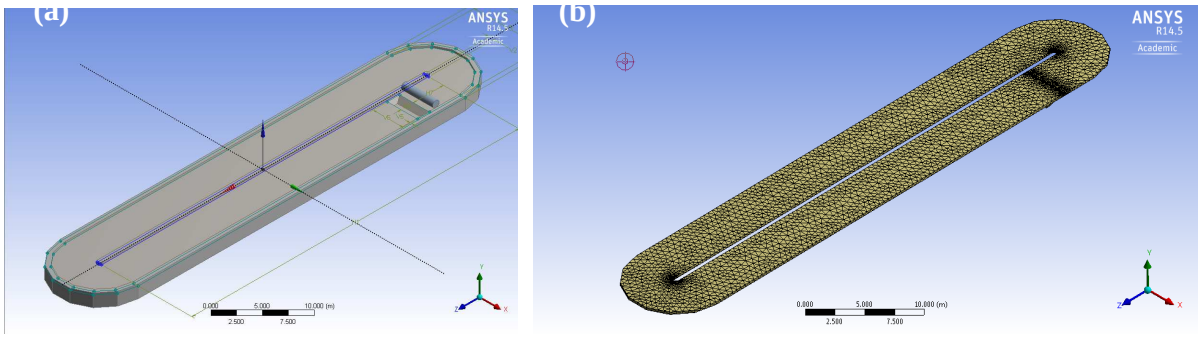

Figure 63. (a) 3-Dimensional representation of pond walls in ANSYS DesignModeler™, and (b) tetrahedral mesh created with the fluid body in ANSYS Meshing™.

The kinetic equations in the previous section were merged with a CFD model using ANSYS® Fluent by using a user-defined function (UDF) written in C. By using user-defined scalars (UDS) created to represent algae mass concentration (X), CO_2 concentration (C), and nitrogen concentration (N) based on the series of kinetic equations in the previous section, the UDF was configured to alter set values inside each individual mesh element throughout the model. After the UDS was set, the UDF was able to access the memory locations and use them to describe X, C, and N in each mesh cell. The UDF was comprised of two main components – an initialization function and adjust function. The initialization function set each variable to an initial value in each cell, and the adjust function manually adjusted each value in an individual cell on every iteration, based on the given equation in the UDF.

Validation

In order to validate the simulation performed in the aforementioned software, the biomass concentration and nitrogen concentration were measured from daily samples taken from the outdoor ponds located at Cedar Lane Farms. The water temperature, irradiance, and CO_2 concentration in the pond were recorded in real time using a CR3000 Micrologger® (Campbell Scientific, Inc., Logan, UT).

Results and Discussion

Figures 64 and 65 show the changes in biomass, CO_2, nitrogen and oxygen in the simulated algae ponds. The diurnal change in temperature and irradiance were taken into account, thus showing the daily 'pulsing' phenomena in the change in biomass, CO_2, and oxygen.

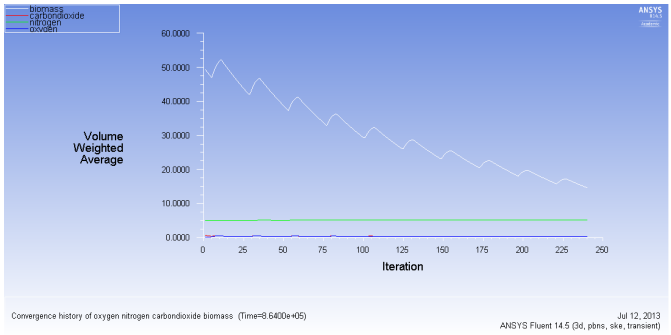

Figure 64. Change in biomass (white), CO_2 (red), nitrogen (green), and oxygen (blue) in the ANSYS simulation of the algae raceway pond

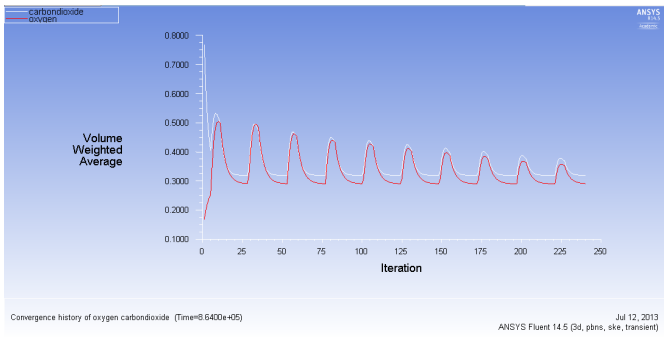

Figure 65. Change in CO_2 (white) and oxygen (red) in a larger scale

Nitrogen appears to be constant in the simulation, which was not the case for the actual data obtained from the ponds. There was a significant decrease apparent in the ponds due to the metabolism of the algal biomass and other life forms present, as shown in **Figure 66**.

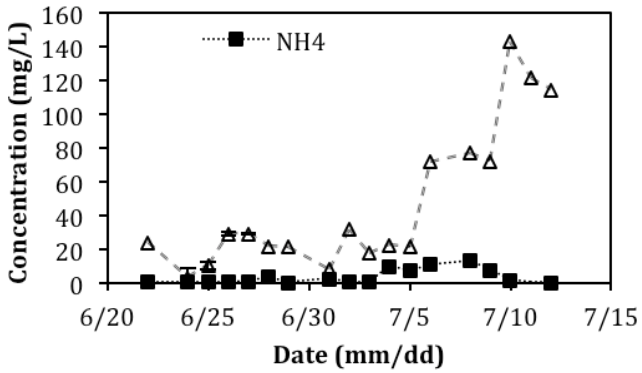

Figure 66. Change in ammonium (NH_4^+) and nitrate (NO_3^-) in open pond

***Nannochloropsis salina* Cultivation in Diluted Anaerobic Digester Effluent under Simulated Seasonal Climatic Conditions**

The purpose of this study was to evaluate the use of anaerobic digester effluent (ADE) for the cultivation of *Nannochloropsis salina* under climatic conditions experienced at pilot scale. The study attempted to compare ADE with traditional commercial nutrients (CN) on algae biomass productivity and nitrogen removal under a variety of light and temperature conditions. The

impact of light exposure (light availability*light intensity) and temperature on algae culture was evaluated. The results showed that light exposure directly impacted this strain's productivity when cultured in either CN or diluted ADE. The nutrient source did not significantly ($\alpha<0.01$) affect biomass productivity, indicating ADE is an adequate nutrient source for *N. salina* in a variable climate. Total nitrogen (TN) removal in diluted ADE increased with rising temperature. Biomass production in 1000-L open raceway ponds can be reasonably predicted from the experimental results.

Materials and Methods

In order to determine the effect of seasonal climatic conditions, 1-L algae cultures were exposed to three light availability conditions (6 h light, 12 h light, 24 h light), three temperature levels (15, 20, 25°C) and two nutrient sources (CN, ADE) at the same TN concentration (200 mg/L). Wastewater characteristics of AD effluent centrate were analyzed and are described in **Table 12**.

Table 12. AD effluent WW analytes (9/11/2012)

Nutrient Constituent	**Concentration (ppm)**
Total Nitrogen	2897 ± 87
Total Phosphorus	425 ± 1
Ammonia Nitrogen	2845 ± 25
Nitrate Nitrogen	9.30 ± 1
TKN	2850 ± 50

In order to include the effect of photosynthetic active radiation or light intensity (LI) on growth, a light exposure (LE) metric was developed:

$$Light\ Exposure(LE) = Light\ Availability\ (LA) * Light\ Intensity\ (LI) * Conversion$$

Biomass growth was measured by daily monitoring of optical density (OD) at 440 nm. The specific growth rate (μ_{net}) was calculated via the equation below:

$$\mu_{net} = \frac{\ln(X_t) - \ln(X_0)}{t}$$

Where:

X_0 = biomass concentration at the beginning of the exponential growth phase

X_t =biomass concentration at the end of the exponential growth phase

t= time period of exponential growth phase (days)

Multiplication of the specific growth rate by the biomass concentration at the end of exponenttial phase (X_t) provides the biomass productivity (Pr) (g L^{-1} d^{-1}).

In order to properly evaluate the effect of temperature, the biomass productivity was divided by average light exposure to establish the Pr/LE index.

Total nitrogen removal was calculated from the equation below:

$$TN\ removal\ (\%) = \frac{TN_t - TN_0}{TN_0}$$

Where:
TN_0= total nitrogen at the beginning of batch cycle
TN_t=total nitrogen concentration at the end of batch cycle

Effect of Light Exposure (LE) on Biomass Productivity (Pr)
Figure 67 shows the effect of light exposure on biomass productivity for cultures grown in diluted anaerobic digester effluent (ADE). **Figure 68** shows the effect of light exposure on biomass productivity for cultures grown in commercial nutrients (CN).

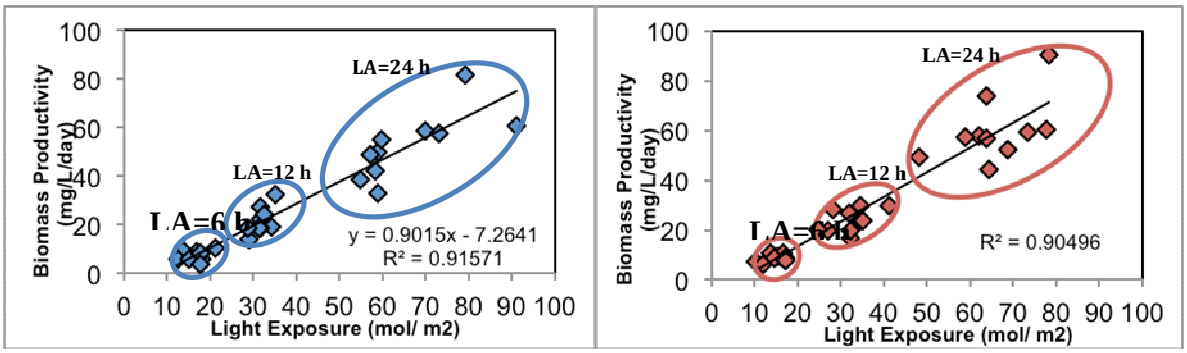

Figure 67 and 68. Effect of light exposure on *N. salina* biomass productivity

As displayed in **Figures 67 and 68**, light exposure significantly impacts biomass productivity in both anaerobic digester effluent (**Figure 67**-left) and commercial nutrients (**Figure 68**-right). When light availability was reduced from 24 to 12 or 6 hours, productivity declined by over 50% or 70%, respectively. Therefore, in outdoor conditions using sunlight as a light source, it can be expected that *N. salina* biomass productivity will be significantly impacted by the season (spring, summer, autumn) of cultivation.

Effect of Temperature on Biomass Productivity (Pr)/Light Exposure (LE).
Figure 69 shows the effect of temperature on biomass productivity/light exposure for cultures grown in either diluted anaerobic digester effluent (ADE) or commercial nutrients (CN).

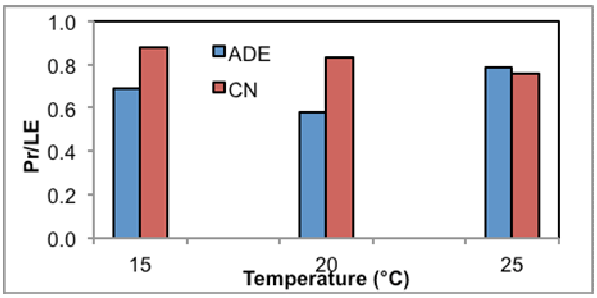

Figure 69. Effect of temperature on average *N. salina* biomass

Productivity/Light Exposure

Figure 69 shows that when the effect of light exposure is held constant, the effect of temperature is minimal over the range tested (15-25°C), indicating that this strain is suitable for Midwest cultivation as long as light is adequately available. The figure also displays commercial nutrients are higher at low temperatures (15 and 20°C), indicating commercial growth media may be more stable in autumn or spring months. However, at 25°C, ADE compared favorably with CN under the conditions tested, indicating ADE can be a suitable nutrient source in summer months.

Effect of Temperature and Light Availability on Total Nitrogen Removal in AD Effluent
Figure 70 shows the effect of temperature and light availability on nitrogen removal (%) in systems cultivated with anaerobic digester effluent.

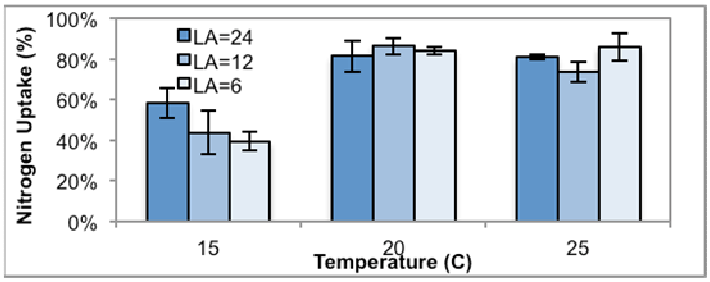

Figure 70. Effects of light availability (LA) and temperature on nitrogen uptake (%)

Figure 70 shows increasing temperature will improve the nutrient removal when cultivating *N.salina* in anaerobic digester effluent. Therefore, if wastewater treatment were attempted in open raceway systems, temperature regulation would be critical to proper removal efficiencies.

Comparison between Laboratory Data and 1000-L Open Raceway Pond (ORP)
Using the light exposure model discussed above and data from the OARDC Weather Station, biomass productivity was predicted for outdoor open raceway ponds. **Figure 71** shows the results from this analysis.

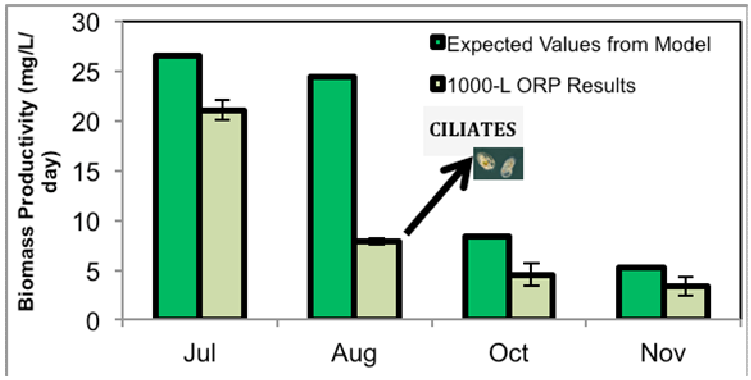

Figure 71. Open raceway/experimental results comparison

Similar productivities were found between the model and actual data. During August, ORP experimental results were substantially affected by predator contaminants. The results indicate light exposure is critical to the success of outdoor open raceway cultivation systems. In a temperate climate, variable light availability will be the most significant factor affecting biomass productivity when temperature is held within the range tested (15-25°C).

As the weather improved, the outdoor Ponds 1 and 2 were inoculated and outdoor algae growth and CO_2 consumption were monitored. Continuous harvesting activities yielded over 200 kg algae dry weight for Ponds 1, 2 and 4. Studies were conducted to determine the effect of anaerobic digestion effluent as a nutrient source and the resulting lipid productivity of the algae. Lipid content and total fatty acids were unaffected by culture system and nutrient source, indicating that open raceway ponds fed diluted AD effluent can obtain similar lipid productivities to open raceway ponds using commercial nutrients.

4.0 Marketing/Commercialization Discussion

Using the *Aquatic Species Program* close-out report as well as the recently published *National Algal Biofuels Technology Roadmap* from DOE, some preliminary estimates of cost savings utilizing the PCM concept may be obtained. Based on a 400 hectare, unlined, brackish water, open-pond system size, the savings that can be attributed to covering substantially all of the surface area of the ponds with the PCM can be estimated as follows:

1. Evaporation of water/day: 400 ha x 2 ft. deep ponds = 650,000,000 gallons of water
   48 inches evaporation/year typical = 2.1 billion gallons/water/year lost to evaporation

   Fresh water make-up cost: 2.1B gallons/year x $400/million gallons = **$840,000/year**

   Salt disposal costs: **$1,200/ha/year avoided**

2. Heating & cooling costs:

The heating and cooling costs for large open-pond systems are not readily calculated because of the significant differences in temperature fluctuations that are site-dependent. Further, it is not economically feasible to provide active heating and cooling to such large volumes of water for algae biofuels production. The means of cooling would be evaporative, requiring large volumes of water pumped from underground aquifers or drawn from rivers – which is not feasible. Fossil-fueled boilers would provide heat and also a ready source of CO_2 that is required for algae production, anyway. However, this approach is not a goal of algae production – to require fossil fuel inputs. Past pilot-scale trials using open ponds in desert climates have reported lower than expected algal productivities due to wide seasonal temperature fluctuations. Thus, a more important measure of the benefits associated with integrating the PCM into a large, open-pond production system is to look at the increase in algal productivity by maintaining more stable temperatures by this passive control. If an increase of approximately 10% in algal productivity could be attributed to the addition of the PCM covering, then use of this material would mean an approximate increase of perhaps 12 metric tons of algae biomass/ha/year. Assuming a biofuel yield of approximately 40 gallons/mt of algae biomass, this would equate to an additional 500

gallons of algae biofuel/ha/year. If the value of the biofuel were assumed to be $2.50/gallon, this would be an increase in revenue of approximately **$1,250/ha/yr.**

3. Invasive species control:
The value of being able to control invasive species is difficult to estimate with any degree of accuracy. However, the benefits are obvious – more algae oil could be produced because lower oil-producing native strains would be greatly diminished, and maintenance costs could be reduced because ponds would not have to be drained, sterilized, and re-inoculated. Thus, a conservative estimate is that 10% more algae oil production could be realized by utilizing the PCM cover to reduce the establishment of invasive strains. Use of the same calculations as above leads to another increase of 500 gallons of biofuel/ha/year.

As indicated below, adding the evaporation water and salt-disposal savings and the increased algae production revenue, it is estimated that approximately ***$2,300,000***/year for a 400 ha size is the benefit that could be realized by incorporating the PCM into commercial-scale open pond algae production.

$840,000 year (water savings) + $1,200 x 400 ha (avoided salt disposal) + $1,250 x 400 ha (heating/cooling effects) + $1,250 x 400 ha (reduction in invasive species) =

$2,320,000 net yearly benefit for a 400 ha system

The cost of the raw material for the PCM is estimated at approximately $5/gallon at commercial quantities. It appears that between 1 to 2 inches of PCM will be all that is required to achieve the thermal performance goals. If only evaporation regulation and invasive species control are the main objectives, then only a thin layer will be required, and much lower material costs can be assumed. Moreover, this method appears to be an attractive solution for the algae biofuels companies that are anticipating using genetically modified strains. The ability to keep the GM algae strain contained within lower-cost open ponds using Touchstone's PCM approach means that photobioreactors may not be needed, further reducing costs with potential increased yields from the GM algae. Heating and cooling control will require more volume of material, and these quantities will need to be more accurately determined in the Phase I demonstration project.

Thus, there appears to be a tremendous opportunity to capture significant value by incorporating the PCM into open-pond production systems. There will be some minor system modifications such as containment dikes around the paddlewheel mixers and a simple system to skim, clean, and re-circulate the PCM as a maintenance consideration. However, the benefits analysis appears attractive and warrants further pilot-testing under this proposed effort.

Touchstone's ongoing technology development in the area of open-pond PCM enhancements and lower-cost algae bioharvesting are aligned to position Touchstone to capture market share in the emerging algae biofuels industry. Commercialization plans are to strategically partner with or license these technologies to leading algae biofuels producers or providers of upstream production technologies. Ideally, non-exclusive license agreements could be established with multiple leading algae producers, along with ongoing royalty payments based on commercial

production of algae oil. Touchstone would provide technology integration expertise, PCM sales, installation and operator training, and ongoing service. Alternatively, Touchstone could provide an exclusive license agreement with one leading algae producer or investor for subsequent commercialization. Either way, Touchstone does not intend to commercialize its algae technologies by owning and operating large-scale algae production facilities, but rather sees itself as an advanced technology supplier to other, currently well-capitalized industry players.

5.0 Conclusions

During this Phase II effort the PCM technology was demonstrated on the pilot scale through direct comparison between test ponds and control ponds. For even a small layer of PCM material, less than 1/8-inch, the average daily water temperature was approximately 3°C higher than the control pond, and the phase transition of the PCM material reduced the daily temperature swings by about 33%. The PCM also resulted in a 74% reduction in water loss compared to the control pond. The PCM pond density was 80% higher than the control pond and also achieved an 80% increase in harvested algae compared to the control pond. These results demonstrate the significant advantages attainable through the use of the PCM technology.

6.0 Final Budget Summation

COST PLAN/STATUS

Baseline Reporting Quarter	YEAR 1 Start: 10/1/09 End: 9/30/10				YEAR 2 Start: 10/1/10 End: 9/30/11				YEAR 3 Start: 10/1/11 End: 9/30/12				YEAR 4 Start: 10/1/12 End: 9/30/13			
	Q1	Q2	Q3	Q4	Q1	Q2	Q3	Q4	Q1	Q2	Q3	Q4	Q1	Q2	Q3	Q4
Baseline Cost Plan (from SF-424A)	(From 424A, Sect. D)				(From 424A, Sect. E)				(From 424A, Sect. E)				(From 424A, Sect. E)			
Federal Share		273,328	244,490	-	130,381	459,486	1,280,334	924,681	465,255	465,255	465,255	465,255	395,910	395,910	395,910	395,910
Non-Federal Share		54,338	75,116	-	21,791	76,803	181,793	108,367	158,180	158,180	158,180	158,180	134,604	134,604	134,604	134,604
Total Planned (Federal and Non-Federal)		327,666	319,606	-	152,172	536,289	1,462,127	1,033,048	623,435	623,435	623,435	623,435	530,513	530,513	530,513	530,513
Cumulative Baseline Cost		327,666	647,272	647,272	799,444	1,335,733	2,797,860	3,830,908	4,454,343	5,077,778	5,701,212	6,324,647	6,855,160	7,385,674	7,916,187	8,446,700
Actual Incurred Costs																
Federal Share		139,640	255,825	122,353	138,020	352,416	556,622	851,766	942,204	795,023	202,462	665,823	598,743	536,253	404,769	166,459
Non-Federal Share		34,910	63,956	41,374	3,365	67,816	83,415	99,821	110,420	199,670	93,968	309,027	277,882	248,891	133,209	12,774
Total Incurred Costs-Quarterly (Federal and Non-Federal)		174,550	319,782	163,727	141,385	420,232	640,037	951,587	1,052,624	994,693	296,430	974,850	876,625	785,144	537,979	179,233
Cumulative Incurred Costs		174,550	494,332	658,059	799,445	1,219,677	1,859,714	2,811,301	3,863,925	4,858,617	5,155,047	6,129,897	7,006,522	7,791,666	8,329,645	8,508,878
Variance																
Federal Share		133,688	(11,335)	(122,353)	(7,639)	107,070	723,712	72,915	(476,948)	(329,768)	262,794	(200,567)	(202,833)	(140,343)	(8,860)	229,451
Non-Federal Share		19,428	11,160	(41,374)	18,426	8,987	98,378	8,546	47,759	(41,491)	64,211	(150,848)	(143,278)	(114,287)	1,394	121,829
Total Variance-Quarterly (Federal and Non-Federal)		153,116	(176)	(163,727)	10,787	116,057	822,090	81,461	(429,189)	(371,258)	327,005	(351,415)	(346,111)	(254,630)	(7,466)	351,280
Cumulative Variance		153,116	152,940	(10,787)	(1)	116,056	938,146	1,019,607	590,418	219,160	546,165	194,750	(151,362)	(405,992)	(413,458)	(62,178)